

Developmental Expression of Neuregulin-3 in the Rat Central Nervous System

Afrida Rahman¹, Janet Weber², Edward Labin³, Cary Lai¹ and Anne L Prieto^{1*}

RUNNING TITLE: Nrg3 in the rat nervous system

¹Dept of Psychological and Brain Sciences, Indiana University, Bloomington, IN.

²Dept. Neuroscience, University of California San Diego, San Diego, CA.

³Department of Neurology, University of Minnesota, Minneapolis, MN.

***Address correspondence to:**

Anne L. Prieto, Dept. of Psychological and Brain Sciences, Indiana University, 1101 East 10th Street, Bloomington, IN 47405, USA.

Telephone: (812) 855-4642, Fax (812) 855-4691 email aprieto@indiana.edu

ACKNOWLEDGMENTS.

We acknowledge the help provided by Dr. Jim Powers at IU Bloomington Light Microscopy Imaging Center with the immunofluorescent microscopy. We also acknowledge the help of Dr. Anna Kalinovsky for the analysis of Nrg1 type III in the cerebellum. We also thank Dr. Shubha Tole for helpful discussions regarding the hem and anti-hem. Also we want to thank Sue Childress and Andrea Hohmann for the use of their cryostats. We also wish to thank Sarah Hocevar, Natalie Wallace and Jeffrey Yu for excellent technical assistance.

This research was also supported by an Indiana University award to Anne L. Prieto and by a major grant from the Lilly Endowment, Inc, Indianapolis, IN to Cary Lai.

This article has been accepted for publication and undergone full peer review but has not been through the copyediting, typesetting, pagination and proofreading process, which may lead to differences between this version and the Version of Record. Please cite this article as doi: 10.1002/cne.24559

© 2018 Wiley Periodicals, Inc.

Received: May 24, 2018; Revised: Aug 24, 2018; Accepted: Oct 11, 2018

ABSTRACT

Neuregulin-3 (Nrg3) is a member of the Nrg family of growth factors identified as risk factors for schizophrenia. There are three Nrgs expressed in the nervous system (Nrg1-3) and of these Nrg1 has been the best characterized. To set the groundwork for elucidating neural roles for Nrg3, we studied its expression in the rat brain at both the RNA and protein levels. Using an antibody developed against Nrg3, we observed a developmental increase of Nrg3 protein expression from embryonic stages to adulthood and determined that it carries O-linked carbohydrates. In cortical neuronal cultures, transfected Neuro2a cells, and brain tissue sections Nrg3 protein was localized to the soma, neurites, and to the Golgi apparatus, where it is prominently expressed. Nrg3 was detected in excitatory, GABAergic and parvalbumin-expressing inhibitory neurons while expression in glia was limited. Nrg3 mRNA and protein were widely expressed during both embryonic and postnatal ages. At E17, Nrg3 was detected within the cortical plate and ventricular zone suggesting possible roles in cell proliferation or migration. At postnatal ages, Nrg3 was abundantly expressed throughout the cerebral cortex and hippocampus. Multiple thalamic nuclei expressed Nrg3, while detection in the striatum was limited. In the cerebellum, Nrg3 was found in both Purkinje cells and granule neurons. In the rodent brain, Nrg3 is the most abundantly expressed of the Nrgs and its patterns of expression differ both temporally and spatially from that of Nrg1 and Nrg2. These findings suggest that Nrg3 plays roles that are distinct from the other Nrg family members.

KEY WORDS: Neuregulin, Nrg3, Golgi apparatus, post translational modifications, protein expression, schizophrenia. RRID: AB_2564462, RRID: AB_2564643, RRID: AB_10000347, RRID: AB_10000343, RRID: AB_2566639, RRID: AB_94872, RRID: AB_398141, RRID: AB_2242334, RRID: AB_141372, RRID: AB_10563748, RRID: AB_2337938, RRID: AB_2338504, RRID: AB_2314501, RRID: MGI: 5651135, RRID: CVCL_0470, RRID: SCR_002368, RRID: SCR_014329, RRID: SCR_013673.

1 INTRODUCTION

Neuregulin-3 (Nrg3) is a member of the neuregulin (Nrg1-4) family of growth factors, which play important roles in the developing and mature nervous system (Birchmeier & Bennett, 2016; Grieco, Holmes, & Xu, 2018; Mei & Nave, 2014; Mei & Xiong, 2008). Nrg3 is of particular interest as it has emerged as a candidate risk gene for several neuropsychiatric disorders including bipolar disorder and schizophrenia (SZ) (Avramopoulos, 2018; P. L. Chen et al., 2009; Hayes et al., 2016; Loos et al., 2014; Paterson et al., 2017). Recent studies have also indicated that Nrg3 plays important roles in cortical development (Bartolini et al., 2017) and glutamatergic neurotransmission (Y. N. Wang et al., 2018). Along with studies on Nrg2 as a regulator of dopaminergic and glutamatergic function (Lee et al., 2015; Vullhorst et al., 2015; Yan et al., 2017), the current evidence supports the concept that Nrgs 1, 2, and 3 perform distinct functions in the central nervous system (CNS). In order to gain an improved understanding of the roles played by these factors in the nervous system, it is essential to characterize their developmental expression patterns. In the present study we set out to provide a comprehensive description of the developmental expression of Nrg3, an understudied Nrg in the rat CNS.

The Nrgs are encoded by four genes, of which three (*Nrg1-3*) are expressed in the CNS (Birchmeier & Bennett, 2016; Carraway et al., 1997; M. S. Chen et al., 1994; Falls, 2003; Falls, Rosen, Corfas, Lane, & Fischbach, 1993; Holmes et al., 1992; X. Liu et al., 2011; Longart, Liu, Karavanova, & Buonanno, 2004; Marchionni et al., 1993; Meyer et al., 1997; Wen et al., 1992; Zhang et al., 1997). They are structurally related and all contain an epidermal growth factor (EGF)-like domain in their extracellular region, which is required to activate members of the ErbB receptor tyrosine kinase family. Although they share these features, the Nrgs (1, 2 and 3) differ in their domain organization, and function. Our current understanding of the biological functions of the Nrgs is complicated by the large number of isoforms that arise as a result of alternative splicing and also by the diversity of post-translational processing events such as

proteolytic cleavage and glycosylation. Among the Nrgs, Nrg1 has been the most extensively characterized and it exhibits the highest level of structural complexity. The *Nrg1* gene gives rise to multiple isoforms of Nrg1 displaying a diversity of structural domains. These have been grouped into six types (I-VI) (Falls, 2003; X. Liu et al., 2011; Steinthorsdottir et al., 2004) including immunoglobulin (Ig)-like domain-containing forms (Nrg1 types I, II, IV and V), the kringle domain forms (Nrg1 type II) or cysteine-rich domain forms (Nrg1 type III). Nrg2 resembles the Ig-like domain containing isoforms of Nrg1, a domain absent from Nrg3 isoforms. Little is known about the alternative splicing of Nrg3 in the rodent, in contrast to its detailed characterization in human (Carteron, Ferrer-Montiel, & Cabedo, 2006; Kao et al., 2010; Paterson et al., 2017; Zeledon et al., 2015). The *Nrg3* human transcripts have been categorized into four major types, shown to be dynamically regulated throughout prefrontal cortical development (Paterson et al., 2017).

Nrg3 resembles Nrg1 type III in its topological organization as it contains two transmembrane domains (TM_N and TM_C) with its N-terminus located in the cytoplasm. Recent work using Nrg3-transfected neurons has shown that BACE1 proteolytically cleaves Nrg3 at a site between the second transmembrane domain (TM_C) and the EGF-like domain (Vullhorst, Ahmad, Karavanova, Keating, & Buonanno, 2017). This yields a transmembrane form of Nrg3 that remains tethered to the membrane via its TM_N domain, giving rise to a structure that permits the EGF-like domain to engage ErbB receptors. This processed form of Nrg3 has been localized to axons, while the unprocessed form has been detected in the soma (Vullhorst et al., 2017).

NRG3 has been associated with an increased risk for SZ, and multiple behavioral and cognitive abnormalities (Avramopoulos, 2018). Genetic studies have reported a consistent relationship between single nucleotide polymorphisms (SNPs) located within the first intron of *Nrg3* and the SZ endophenotype of delusional behavior (Morar et al., 2011). The characterization of Nrg3^{-/-} mice further revealed behaviors that are consistent with animal

models of SZ, showing increased levels of novelty-induced hyperactivity, impaired pre-pulse inhibition and a reduction in fear conditioning (Hayes et al., 2016). Increased levels of Nrg3 expression in mice correlate with impulsivity, with the opposite effect seen in Nrg3-deficient mice (Loos et al., 2014). Paterson and Law (Paterson & Law, 2014) also reported that injection of Nrg3 at an early postnatal age resulted in increased anxiogenic-like behavior and reduced sociability in adult mice. In at least two studies (Meier et al., 2013; Morar et al., 2011), NRG3 variants have also been associated with attention deficits observed in SZ. Other studies have also linked specific NRG3 SNPs with increased risk for Alzheimer's disease (K. S. Wang et al., 2014) and nicotine dependence (Turner et al., 2014; Zhou et al., 2018).

An improved understanding of Nrg3 signaling at the cellular and systems level should continue to provide insights into how its dysregulation contributes to these neuropathological conditions. A recent study has identified Nrg3 as a regulator of glutamatergic neurotransmission (Y. N. Wang et al., 2018). Deletion of Nrg3 in pyramidal neurons resulted in enhanced neurotransmission as evidenced by an increase in glutamate release. Increased levels of Nrg3 led to the opposite result with a decrease in glutamatergic neurotransmission. These observations provide one mechanism to explain how alterations in Nrg3 mRNA levels (Kao et al., 2010; Paterson et al., 2017) underlie changes in glutamatergic neurotransmission associated with these pathological conditions (Cappellini et al., 2006; Gao & Penzes, 2015).

Studies in rodent and human have provided evidence that Nrg3 is involved in cortical development and function. The earliest reported expression of Nrg3 is at embryonic (E) day 12.5 in the anti-hem, a structure in the lateral neuroepithelium that gives rise to the cerebral cortex (Assimacopoulos, Grove, & Ragsdale, 2003). At E16, Zhang et al (Zhang et al., 1997) observed that Nrg3 was predominantly expressed in neural tissue with high levels detected in the cortical plate. A recent effort has provided a detailed characterization of Nrg3 expression throughout early cortical development (E13.5 to P4) (Bartolini et al., 2017). These investigators have determined that Nrg3 serves to regulate the migration of interneuronal precursors into

distinct cortical layers. Although the information regarding Nrg3 expression in the postnatal period is more limited (Anton et al., 2004; Longart et al., 2004), it is evident that Nrg3 is more widely expressed than either Nrg1 type III or Nrg2.

In order to provide a framework for future studies on Nrg3 function in the CNS, we have sought to provide a comprehensive analysis of the spatiotemporal distribution of Nrg3 mRNA and protein in the embryonic and postnatal rat brain. We have observed that Nrg3 is widely expressed throughout the CNS during both embryonic and postnatal ages. Expression is largely confined to neurons with low to background levels detected in white matter tracts. We further characterized the subcellular localization of Nrg3 in Neuro2a cells and cortically-derived cell cultures. In neurons, Nrg3 was localized to the plasma membrane of the cell soma, neurites, and Golgi apparatus. In glia, Nrg3 detection was limited to the Golgi apparatus. Nrg3 was highly expressed and widely distributed in the brain, compared to Nrg1 type III and Nrg2. Our observations are consistent with and extend those of Longart *et al* (Longart et al., 2004), Anton *et al* (Anton et al., 2004) and Bartolini *et al* (Bartolini et al., 2017). Our findings have identified regions throughout the rodent CNS in which Nrg3 may play functional roles and highlight potential cellular model systems to study Nrg3 in health and disease.

2 MATERIALS AND METHODS

2.1 Antibody characterization and reagents. Antisera #4116 against Nrg1, #4122 against Nrg2, and #6144 against Nrg3 were generated in house, affinity-purified, and tested for their specificity as described in detail below. Commercial antibodies were obtained from the following sources: mouse monoclonal anti-glial fibrillary acidic protein (GFAP) raised against recombinant human GFAP (BioLegend, San Diego, CA, Cat# 672402, RRID: AB_2564462); mouse monoclonal anti-microtubule-associated protein 2 (MAP2) raised against mammalian MAP2 (BioLegend, Cat# 801801, RRID: AB_2564643); mouse monoclonal anti-calbindin D-28k

produced by hybridization of mouse myeloma cells with mouse spleen cells raised against chicken calbindin D-28k (Swant, Marly, Switzerland, Cat# 300, RRID: AB_10000347); mouse monoclonal anti-parvalbumin produced by hybridization of mouse myeloma cells with mouse spleen cells raised against parvalbumin purified from carp muscles (Swant, Cat# 235, RRID: AB_10000343); mouse monoclonal anti-myelin 2',3'-cyclic-nucleotide 3'-phosphodiesterase (CNPase) raised against human myelin CNPase (BioLegend, Cat# 836404, RRID: AB_2566639); mouse monoclonal anti-O4 clone 81 produced using homogenate of white matter of corpus callosum from bovine brain (EMD Millipore, Burlington, MA, Cat# MAB345, RRID: AB_94872); mouse monoclonal anti-Golgi matrix protein of 130 kDa (GM-130) raised against amino acids 869-982 corresponding to rat GM-130 (BD Biosciences, San Jose, CA, Cat# 610822, RRID: AB_398141); mouse monoclonal anti- β -actin raised against a synthetic peptide corresponding to amino-terminal residues of human β -actin (Cell Signaling Technology, Danvers, MA, Cat# 3700, RRID: AB_2242334); polyclonal Alexa Fluor 594 goat anti-mouse raised against gamma immunoglobulins (Ig) heavy and light chains (Thermo Fisher Scientific, Waltham, MA, Cat# A-11005, RRID: AB_141372); polyclonal Alexa Fluor 488 goat anti-rabbit raised against gamma Ig heavy and light chains (Thermo Fisher Scientific, Cat# A-11008, RRID: AB_10563748); polyclonal horse radish peroxidase (HRP) conjugated goat anti-rabbit IgG raised against Ig heavy and light chains (Jackson ImmunoResearch Labs West Grove, PA, Cat# 111-035-045, RRID: AB_2337938); and polyclonal HRP conjugated goat anti-mouse IgG raised against Ig heavy and light chains (Jackson ImmunoResearch Labs Cat# 115-035-062, RRID: AB_2338504). The anti-GAD-6 monoclonal antibody specific against rat GAD-65 (Developmental Studies Hybridoma Bank (DSHB) Cat# GAD65, RRID: AB_2314501) was developed by David Gottlieb (Washington University School of Medicine St. Louis, MO). It was obtained from the DSHB developed under the auspices of the Eunice Kennedy Shriver National Institute of Child Health and Human Development (NICHD) and maintained by The University of Iowa, Department of Biological Sciences. All antibody dilutions are reported in the section

where their use is described. To test for specificity of secondary antibodies during immunolabeling experiments, negative controls were included to detect any non-specific binding of the secondary antibodies or background fluorescence. Negative controls followed the same immunolabeling procedures omitting incubation with primary antibodies.

2.2 Animals. Sprague Dawley rats (Envigo, Indianapolis, IN, Cat # Sprague Dawley SD # 002, RRID: MGI: 5651135) were used for *in situ* hybridization, immunohistochemistry, immunocytochemistry, and Western blotting experiments. Rat embryos of day 17 or 18 were used to prepare primary cortical cultures, as described below. Both embryonic (E) and postnatal (P) rats were utilized for Western blotting, immunohistochemistry, and *in situ* hybridization experiments. Depending on the experiment, pregnant and postnatal rats were euthanized by CO₂ inhalation. Embryos were removed via caesarian section to obtain primary cortical cultures. For immunohistochemistry and *in situ* hybridization, postnatal rats were first anesthetized prior to perfusion (as described in detail below). For all experiments in which animals were involved, including immunizations, we followed guidelines established by the NIH Guide for the Care and Use of Laboratory Animals and a protocol approved by The Scripps Research Institute Institutional Animal Care and Use Committee and also approved by the Indiana University Institutional Animal Care and Use Committee.

2.3 Fusion proteins and cDNA constructs. Glutathione-S-transferase (GST) fusion proteins encoding the epidermal-growth factor (EGF)-like domain and flanking regions of Nrg1, Nrg2, and Nrg3 were generated in house, and used for antibody production and purification. Information regarding the production of Nrg1 and Nrg2 fusion proteins was previously published in Ghashghaei *et al.*, 2006 (Ghashghaei et al., 2006). Nrg3 fusion proteins were generated using polymerase chain reaction (PCR) to amplify a region corresponding to the Nrg3 EGF-like domain cassette region between base pairs 1132-1368 in accession number NM_001190187.1

corresponding to murine Nrg3 reference sequence (variant 2). This amplified sequence corresponds to amino acids:

SEHFKPCRDKDLAYCLNDGECFVIETLTGSHKHCRCKEGYQGVRCDQFLPKTDSILSDPTDHLGIEFMESEDVYQR. The PCR products were subcloned into the pGEX-6P-2 vector (GE Healthcare Bio-Sciences Pittsburgh, PA). After nucleotide sequence verification, the recombinant constructs or the unmodified vectors were transformed into the Origami strain of *E. coli* (EMD Millipore, Burlington, MA) and used for fusion protein production and purification (Nrg3-GST and GST) as previously described in detail in Ghashghaei *et al* (Ghashghaei *et al.*, 2006).

For some experiments we used pcDNA3-CAG-mCherry (a gift from Drs. Kenneth Mackie and Hui-Chen Lu) to visualize the transfected cells as described in the section entitled **Cell Transfection**).

2.4 Generation and purification of anti-Nrg antibodies. The anti-Nrg1 (#4116), Nrg2 (#4122), and Nrg3 (#6144) antisera were raised in rabbits by the subcutaneous injection of GST-Nrg fusion proteins, in complete Freund's adjuvant, followed by booster injections in incomplete Freund's every 3 weeks closely following the protocol described in Prieto *et al.* (Prieto, Weber, & Lai, 2000). Anti-Nrg1-3 antibodies were affinity-purified by passing the #4116, #4122, and #6144 sera through GST, GST-Nrg1, GST-Nrg2, or GST-Nrg3 -Sephrose 4B columns prepared by covalently coupling the proteins to CN-Br Sepharose (GE Healthcare Bio-Sciences) following the purification protocol described in detail in Prieto *et al* (Prieto *et al.*, 2000). The immunoreactivities of the antibodies were tested by immunocytochemistry, immunohistochemistry and Western blot analyses, as described below.

2.5 Preparation and maintenance of cell cultures. Neuro2a (N2a) neuroblastoma cells were obtained from American Tissue Culture Collection (ATCC, Manassas, VA Cat# CCL-131, RRID: CVCL_0470). In order to test the specificity of #6144 serum and the Nrg1-3 affinity-purified antibodies, untransfected N2a cells or cells transiently transfected with Nrg1 (N2a/Nrg1), Nrg2 (N2a/Nrg2), or Nrg3 (N2a/Nrg3) full length cDNAs or also co-transfected with mCherry cDNAs, (N2a/Nrg1/mCherry, N2a/Nrg2/mCherry, N2a/Nrg3/mCherry) were used to prepare detergent extracts (see below under **Cell transfection** and **Western blotting and sample preparation**). The N2a, N2a/Nrg, and N2a/Nrg/mCherry expressing cells were grown in Dulbecco Modified Eagle's Minimal Essential Medium (DMEM, Thermo Fisher Scientific), containing 10% fetal calf serum (FCS, Atlanta Biologicals, Flowery Branch, GA), L-glutamine (2 mM), penicillin (100 U/ml), and streptomycin (100 µg/ml), all from Thermo Fisher Scientific.

Primary cortical cultures were prepared and maintained as previously described in detail in Prieto *et al* (Prieto, O'Dell, Varnum, & Lai, 2007). Cells were plated (8×10^4 cells/well) on 12 mm glass coverslips coated with 250 µg/mL poly-L-lysine in media containing Neurobasal, B-27, penicillin 100 U/mL/streptomycin 100 µg/ml, 0.5 mM L-glutamine, and 0.025 mM L-glutamate (all from Thermo Fisher Scientific). Half of the media was replaced every 4 days with media without glutamate. The cells were cultured for 8 days for immunocytochemistry. Cells were prepared for immunostaining as described in the section **Immunocytochemistry**.

2.6 Cell transfection. For the preparation of detergent extracts using N2a cells expressing Nrgs, N2a cells were plated in 6 well plates at a density of 5×10^5 cells/well and transfected with 2 µg of Nrg plasmids DNA/well. For immunocytochemistry, the cells were plated at a density of 5×10^4 cells/well in 24 well plates and transfected with Nrg plasmid DNAs (0.5 µg/well), or for the doubly transfected cells, with a mixture of Nrg DNA (0.25 µg/well) and mCherry encoding plasmid (0.125 µg/well). For all experiments, the transfections were performed 24 hrs post-plating, using Lipofectamine Plus following manufacturer instructions (Thermo Fisher Scientific).

The cells were grown for 48 hrs before preparation of detergent extracts or fixation for immunocytochemistry.

To determine whether our anti-Nrg3 antibodies cross-react with Nrg1 and Nrg2 in our immunostaining studies, we performed three independent experiments, co-transfecting N2a cells with Nrg1/mCherry, Nrg2/mCherry, and Nrg3/mCherry plasmids on three coverslips per experiment. We imaged five fields within each of the three coverslips having an average of 314 ± 74 cells/field for Nrg1, 205 ± 32 cells/field for Nrg2, and 309 ± 24 cells/field for Nrg3. We also counted the mCherry positive (+), Nrg3 (+) and mCherry/Nrg3 (+) cells on each field and calculated averages for all three experiments. The data are presented as the means and standard deviations of three experiments for each condition. For the Nrg3/mCherry transfections $80.3 \pm 3.0\%$ of the mCherry positive cells also expressed Nrg3 (23.9 ± 1.1 mCherry (+) cells per field and 19.2 ± 1.2 Nrg3 (+) cells per field for all three experiments). We did not detect any anti-Nrg3 (+) cells on the Nrg1/mCherry transfections (23.5 ± 3.2 mCherry (+) cells per field and 0 Nrg3 (+) cells per field for all three experiments). As observed for the Nrg1 transfectants, we did not detect any Nrg3 (+) cells in the Nrg2/mCherry transfections (14.9 ± 1.9 mCherry (+) cells per field and 0 Nrg3 (+) cells per field for all three experiments). To verify that the lack of anti-Nrg3 immunoreactivity in the Nrg1 and Nrg2 transfectants was not due to lack of expression of these polypeptides, we performed a parallel transfection experiment with Nrg1/mCherry, Nrg2/mCherry, and Nrg3/mCherry, and performed Western blotting as described below. We observed clear expression of Nrg1, Nrg2 and Nrg3 in these samples (data not shown).

2.7 Western blotting and sample preparation. Western blotting was performed as previously described in Prieto *et al* (Prieto et al., 2000). Whole brain extracts were prepared for the developmental time course and positive controls from E18, P0, P3, P5, P7, P11, P14, P20, P28, and adult Sprague Dawley rats. Samples were homogenized using a Polytron in lysis buffer

consisting of 50 mM Tris HCl (pH 7.5), 150 mM NaCl, 500 mM EDTA, 0.5 mM Na-orthovanadate, 50 mM NaF, 5 mM $\text{Na}_4\text{P}_2\text{O}_7$, 0.5% NP-40, 1% Triton X-100, 0.1% SDS, and protease inhibitor tablet (Roche Diagnostics Corporation, Indianapolis, IN). To characterize the #6144 antiserum, detergent extracts using the above described lysis buffer were prepared from untransfected or Nrg1, 2, and 3 transfected N2a cells. For some experiments, Nrg transfected N2A cells were also co-transfected with mCherry as described above. Brain and cell lysates were subjected to SDS-PAGE using 8% or 4-20% gradient Tris-glycine gels (Thermo Fisher Scientific) followed by transfer to Immobilon P membranes (EMD Millipore). Following transfer, the membranes were incubated for 30 min in blocking buffer consisting of 10 mM Tris-HCl (pH 7.5), 150 mM NaCl, 0.1% Tween-20 (TBST), and 3% skim milk (Carnation, Nestle, Vevey Switzerland). The membranes were incubated overnight at 4°C in the presence of primary antibody. The following antibodies were used for the Western blot analyses: affinity-purified anti-Nrg1 (0.27 $\mu\text{g}/\text{mL}$), affinity-purified anti-Nrg2 (0.28 $\mu\text{g}/\text{mL}$), affinity-purified anti-Nrg3 (0.27 $\mu\text{g}/\text{ml}$), anti-Nrg3 serum #6144 (1:2,000 dilution) and anti- β -actin (1:10,000). For experiments including pre-absorption, serum #6144 (1:2,000) and affinity-purified anti-Nrg3 (0.27 $\mu\text{g}/\text{ml}$) were resuspended in 10 mLs of blocking buffer in the presence or absence of 1.46 μg GST-Nrg3 and incubated overnight at 4°C. Following pre-absorption the membranes were incubated further overnight with the absorbed or control antibodies. After the overnight incubation with the primary antibodies, the membranes were washed 5 times for 5 min with TBST, blocked for 15 min as described above, and then incubated for 60 min with either horse-radish peroxidase (HRP) conjugated goat anti-rabbit IgG or HRP conjugated goat anti-mouse IgG (1:15,000). The blots were washed 5 times for 5 min with TBST, and processed for chemiluminescence using Super Signal West Pico Chemiluminescent Substrate ECL system (Thermo Fisher Scientific) according to instructions provided by the manufacturers.

2.8 Deglycosylation. Detergent extracts were prepared from E18 and P25 rat cortices in lysis buffer (described above) lacking SDS. Protein corresponding to 30 µg were treated overnight at 37°C with 500 units of N-glycosidase F (PNGase F), Endoglycosidase H (Endo H), O glycosidase (O-gly), or O gly/Neuraminidase (NA) mixture using the conditions and reagents provided by the manufacturers (New England Biolabs, NEB, Beverly, MA). The reactions were stopped by the addition of 2 x Laemmli sample buffer, denatured for 3 min at 98°C, and analyzed by SDS-PAGE as described in **Western blotting and sample preparation**.

2.9 Immunocytochemistry. Primary cortical neurons from E17-18 Sprague Dawley rats (80,000 cells/well) and untransfected N2a, N2a/Nrg cells (50,000 cells/well), or N2a/Nrg/mCherry cells (50,000 cells/well) were seeded onto 12 mm glass coverslips (Thermo Fisher Scientific) coated with 250 µg/mL of poly-L lysine (EMD Millipore). The cells were fixed with cold 4% paraformaldehyde/4% sucrose/PBS for 20 min followed by 5 washes of 5 min each with cold PBS. The cells were blocked for 30 min with blocking buffer consisting of 5% goat serum (Colorado Serum, Denver, CO), 5% fetal calf serum (FCS) (Atlanta Biologicals) in PBS and with or without 0.01% Triton X-100. The cells were incubated overnight at 4°C with the following primary antibodies: serum #6144 (1:250), affinity-purified anti-Nrg3 (2.14 µg/mL), anti-GFAP (1:500), anti-O4 (1:1,000), anti-MAP2 (1:1,000), anti-GAD-6 (1:25,000), and anti-GM-130 (1:500). The cells were then washed 5 times for 5 min in PBS, and further blocked for 30 min. The cells were incubated with Alexa 488-labeled goat anti-rabbit antibodies for the Nrg3 antibodies and Alexa 594-labeled goat anti-mouse antibodies for the mouse antibodies (1:300 dilution in blocking buffer). Cells were incubated at room temperature for 90 min in the dark, and then washed 2 times for 5 min in PBS, and incubated for 10 minutes in PBS/10 µg/mL 4'-6-diamidino-2-phenylindole (DAPI, EMD Millipore) or Hoechst 33342 in PBS/1 µg/mL. (Thermo Fisher Scientific) to visualize the cell nuclei. The cells were further washed 3 times for 5 min with PBS, and then mounted onto glass slides using SlowFade Antifade (Thermo Fisher

Scientific). The cells were photographed under epifluorescence, with immunofluorescence considered to be at background level when the intensity of the signal (very low) matched that observed when only secondary antibodies were used. A subset of images were acquired using a Nikon TE2000 inverted microscope and BD CARVII White light confocal imaging system equipped with a Cascade 16 bit CCD camera. The images were generated using the Universal Imaging Corporation Metamorph 6.1 software package (Universal Imaging, Bedford Hills, NY, <http://www.moleculardevices.com/Products/Software/Meta-Imaging-Series/MetaMorph.html>, RRID: SCR_002368). Other images were acquired using a Nikon NiE upright microscope and Lemuncor SpectraX light source for fluorescence imaging equipped with a Hamamatsu Orca-Flash 2.8 sCMOS high resolution camera. The images were generated using the Nikon Elements software, (Nikon Instruments, <http://nikoninstruments/Products/Software>, RRID: SRC_014329). The images were not modified other than relative adjustments of brightness, contrast, and magnification.

2.10 Immunohistochemistry. Coronal and sagittal sections for immunohistochemistry were prepared from E17, P3, P4, P7, and P20 Sprague Dawley rats. The brains from E17-E19 rat embryos were dissected after removal from the pregnant females, and fixed in 4% paraformaldehyde in PBS. Postnatal rats were first anesthetized with urethane and then transcardially perfused for 2-5 min with 0.1M PB (pH 7.2) followed by 4% paraformaldehyde in PB for 20 min. After dissection, the tissues were further fixed in 4% paraformaldehyde for 4 hrs and equilibrated successively in 15% and 30% sucrose in dH₂O for cryoprotection. In preparation for sectioning, tissues were frozen in dry ice and embedded in Tissue-Tek optimum cutting temperature (O.C.T) medium (Sakura, AJ Alphen aan den Rijn, The Netherlands). Cryostat sections of 15 μ m were collected onto chrom-alum coated slides. Prior to staining, the fixed sections were hydrated in PBS for 10 min and incubated for 30 min at room temperature with blocking buffer (as described in the section **Immunocytochemistry**) containing either

0.01% Triton X-100 or 0.1% saponin. The #6144 serum (1:250), anti-MAP2 (1:1,000), anti-GFAP (1:500), anti-GM-130 (1:500), anti-parvalbumin (1:1,000), anti-CNPase (1:5,000), and anti-calbindin (1:1,000) were diluted in blocking buffer, applied to the tissue sections, and incubated overnight at 4°C. The procedure and visualization for immunohistochemistry closely followed the protocol described in the section **Immunocytochemistry**. Slides were mounted with 50 x 22 mm cover glass (Thermo Fisher Scientific) using SlowFade Antifade. A subset of images were collected using a Nikon TE2000 inverted microscope (as described above). Confocal images were collected using a Leica SP5 Scanning Confocal with a DMI 6000 CS inverted microscope platform and controlled by Leica LAS AF Image Acquisition Software, (Leica Microsystems, <https://www.leica-microsystems.com>, RRID:SCR_013673). The images were not modified other than adjustments of brightness, contrast, and magnification.

2.11 *In situ* hybridization. Coronal and sagittal tissue sections for hybridization were prepared from Sprague Dawley rats of ages E17, E19, P3, P7, P20, and P25. Embryos were removed via cesarean section and fixed in 4% paraformaldehyde in 0.1M sodium borate buffer, pH 9.5. Postnatal rats were first deeply anesthetized with Nembutal and then transcardially perfused with 4% paraformaldehyde in 0.1M sodium borate buffer, pH 9.5. A 766 bp Nrg1 (type III) cDNA fragment (bp 555-1321 in accession #AF194438) and a 750 bp Nrg2 cDNA fragment (bp 586-1336 in accession #D89996) were amplified and subcloned into EcoRI/BamHI cut pBluescript(-). The plasmids were linearized with EcoRI to generate antisense RNAs using T3 RNA polymerase. A 563 bp Nrg3 cDNA fragment (bp 940-1503 in accession #NM_008734) was amplified and subcloned into pCR2.1. The plasmid was linearized with HindIII to generate antisense primers using T7 RNA polymerase. Transcriptions were performed using 125 Ci ³³P-UTP (2,000-4,000 Ci/mole, either NEN or ICN). The pre- and post-hybridization procedures closely followed those of Simmons *et al.* (Simmons, Arriza, & Swanson, 1989). Following these procedures, the slides were passed through dehydration steps prior to dipping into photographic

emulsion and exposed between 7-20 days followed by development and previously described in Prieto *et al.* (Prieto, Weber, Tracy, Heeb, & Lai, 1999). Hybridization signals were considered background when accumulation of silver grains were not associated with a particular area in the tissue and when the distribution of the grain appeared uniform both under dark field and bright field illumination. The hybridization signals were visualized with an Olympus BX51 microscope and photographed using a Nikon Coolpix 4300 digital camera. Images were converted to black and white and were not modified other than relative adjustments to brightness, contrast and magnification.

3 RESULTS

3.1 Characterization of anti-Nrg3 antibodies.

To study the spatio-temporal expression of Nrg3 in the rat nervous system, we raised antibodies (serum #6144) against epitopes contained in the epidermal growth factor (EGF)-like domain and adjacent sequences of Nrg3. We characterized the ability of these antibodies to recognize Nrg3 by Western blotting, immunocytochemistry, and immunohistochemistry.

We first tested their ability to recognize Nrg3 by Western blotting on detergent extracts from untransfected Neuro2a (N2a) cells (U in Figs. 1a and b), N2a cells transfected with Nrg3 (N2a/Nrg3) cells (N3 in Figs. 1a and b), and from adult rat brain homogenates (Br in Fig. 1a). We tested both serum 6144 (Fig. 1a, panels 1 and 2) and affinity-purified anti-Nrg3 from serum 6144 (Fig. 1a, panels 3 and 4, Fig. 1b panel 3). The 6144 serum reacted with a major band of approximately 80 kDa in the N2a/Nrg3 samples (Fig. 1a, panel 1, lane N3) which was absent in the untransfected cells (Fig. 1a, panel 1, lane U) and a band of approximately 97 kDa in the brain extracts (Fig. 1a, panel 1, lane Br). The affinity-purified Nrg3 antibodies, also reacted with the 80 kDa band in the N2a/Nrg3 extracts and a 97 kDa band in the brain extracts (Fig. 1a, panel 3, lane N3 and Br respectively). A minor band of approximately 90 kDa was detected by

serum 6144 in both untransfected and Nrg3 transfected N2a samples (Fig. 1a, panel 1, lanes U and N3) but was not detected even at long exposures when testing the affinity-purified antibodies (Fig. 1a, panel 3). Preabsorption of the 6144 serum (Fig. 1a, panel 2) and affinity-purified antibodies (Fig. 1a, panel 4) with the immunizing antigen (GST-Nrg3) eliminated the immunoreactivity to all bands. The inability to detect additional bands in the N2a/Nrg3 cell and brain extracts indicate that these antibodies specifically recognize Nrg3.

To determine if the anti-Nrg3 antibody cross-reacts with Nrg1 and/or Nrg2, we prepared detergent extracts of N2a cells transfected with cDNAs encoding Nrg1, Nrg2, and Nrg3 (N1, N2, N3 respectively in Fig. 1b, panels 1, 2 and 3). To demonstrate that Nrg1 and Nrg2 are expressed in cell extracts derived from N2a/Nrg1 and N2a/Nrg2 transfected cells, we blotted with affinity-purified anti-Nrg1 antibodies (Fig. 1b, panel 1) and affinity-purified anti-Nrg2 antibodies (Fig. 1b, panel 2). The anti-Nrg1 antibodies (Fig. 1b, panel 1) recognized several bands in the Nrg1 (N1 lane) extract but did not react with bands in the Nrg2 (N2 lane) or the Nrg3 (N3 lane) transfected cells. Similarly, the anti-Nrg2 antibodies (Fig. 1b, panel 2) recognized a major band of approximately 110 kDa and several minor bands in the Nrg2 (N2 lane) transfected cells and an unspecific band of approximately 50 kDa in all cell extracts. Anti-Nrg2 antibodies did not detect any major bands with molecular weights corresponding to either Nrg1 or Nrg3 (Fig. 1b, panel 2 lanes N1 and N3 respectively). When the affinity-purified anti-Nrg3 antibodies were tested (6144) (Fig. 1b, panel 3), they recognized a major band of 80 kDa in the N2a/Nrg3 (N3 lane) cell extracts but did not cross-react with bands corresponding to Nrg1 and Nrg2 (Fig. 1b, lanes N1 and N2). These results indicate that the anti-Nrg3 antibodies are specific for Nrg3 and do not cross-react with Nrg1 or Nrg2 by Western blotting.

To establish a developmental time frame of Nrg3 expression, we used detergent extracts prepared from whole embryonic (E) day 18 to adult (A) rat brains (Fig. 1c) to perform Western blotting using the anti-Nrg3 affinity-purified antibodies. At embryonic and early postnatal stages, relatively low levels of Nrg3 were detected compared to later stages. Nrg3 expression

increased steadily between P0 and P11, a period consistent with a potential role in dendritic elaboration and synaptogenesis (Aghajanian & Bloom, 1967). Nrg3 expression peaked at P14 and remained high throughout adulthood.

We also explored the glycosylation state of Nrg3 since it has a mucin-like region enriched in serine and threonine residues, which can potentially be O-linked glycosylated (Hanisch, 2001; Tran & Ten Hagen, 2013; Zhang et al., 1997). We used enzymes having de-glycosylating activities to monitor changes in the molecular weight of Nrg3 in cortical E18 and P25 extracts. As shown in Fig. 1d, panel 1, treatment of E18 cortical extracts with a combination of O-glycosidase and neuraminidase resulted in a small but noticeable reduction in molecular weight. No significant reductions in molecular weight were observed for treatments using only one of the two enzymes. In contrast, treatment of P25 cortical extracts (Fig. 1d, panel 2) with a combination of O-glycosidase and neuraminidase resulted in a significant molecular weight reduction in Nrg3 from approximately 80 kDa to approximately 60 kDa. This molecular weight reduction was greater than the decrease caused by treatment with neuraminidase alone, which also was significant. In contrast, N-Glycosidase F (PNGase F) and Endoglycosidase H (Endo-H), which act on N-linked sugars, had no effect on Nrg3's molecular weight. This is consistent with the absence of N-linked glycosylation sites in the Nrg3 amino acid sequence (Zhang et al., 1997). These results support the conclusion that Nrg3 is O-linked glycosylated and that its glycosylation state changes over the course of development.

3.2 Compartmentalization of Nrg3 by immunocytochemistry

To determine the subcellular localization of Nrg3, we compared the immunoreactivity of the Nrg3 antibodies on N2a cells transfected with Nrg3 (N2a/Nrg3 in Fig. 2) and untransfected N2a cells (UNT in Fig. 2). Because Nrg3 is a transmembrane protein (Bai et al.; Vullhorst et al., 2017), we performed immunocytochemistry both in the absence (Fig. 2, a-h and i-q) and presence of detergent (0.01% Triton X-100) (Fig. 2, a"-h" and i"-q"). Nrg3 immunoreactivity with

serum 6144 in the absence of detergent (Fig. 2, b, c, o and q) was detected on the plasma membrane of N2a/Nrg3 cells of both the soma and processes. Consistent with these observations, the affinity-purified anti-Nrg3 antibodies also stained the plasma membrane and cell processes (Fig. 2, f and g). In the presence of detergent, the cell surface staining was less evident while the cytoplasmic staining became more pronounced with strong perinuclear Nrg3 immunoreactivity with both serum 6144 (Fig. 2, b", c", o" and q") and the affinity-purified anti-Nrg3 antibodies (Fig. 2, f" and g"). The Nrg3 staining was eliminated when serum 6144 (Fig. 2, d and d") and the affinity-purified anti-Nrg3 (Fig. 2, h and h") were pre-absorbed with the immunizing antigen (GST-Nrg3), both in the absence and presence of detergent. In contrast, untransfected N2a cells were only weakly stained by the 6144 antiserum (Fig. 2, a and a") in the presence and absence of detergent. N2a/Nrg3 transfected cells incubated with secondary antibody alone showed very low background fluorescence under both detergent conditions (Fig. 2, e and e").

To determine if the anti-Nrg3 antibody cross-reacts with Nrg1 or Nrg2 by immunocytochemistry, we compared the immunoreactivity of the Nrg3 serum 6144 on N2a cells transfected with cDNAs encoding Nrg1 (Fig. 2, i-k and i"-k"), Nrg2 (Fig. 2, l-n, and l"-n") or Nrg3 (Fig. 2, o-q, and o"-q"). We also co-transfected with a cDNA encoding mCherry to visualize the transfected cells (Fig. 2, j, j", m, m", p and p"). We performed the immunocytochemistry both in the absence (Fig. 2, i-q) and presence (Fig. 2, i"-q") of detergent (0.01% Triton X-100). Nrg3 immunoreactivity was only detected in the cells transfected with Nrg3 (Fig. 2 o-q and o"-q"). Nrg3 immunoreactivity was not observed in the N2a/Nrg1/mCherry (Fig. 2, i-k and l"-k") or in the N2a/Nrg2/mCherry expressing cells (Fig.2, l-n and l"-n") above that observed in the untransfected cells (Fig. 2, a and a"). We also tested the specificity of our affinity-purified anti-Nrg3 in these experiments and obtained the same results as the 6144 serum (not shown). We also performed a parallel transfection experiment analyzed by Western blotting that allowed us to determine that there was expression of Nrg1, Nrg2 and Nrg3 in these transfectants (data not

shown). These observations allow us to conclude that our anti-Nrg3 antibodies do not cross-react with Nrg1 and Nrg2 both by Western blotting (Fig. 1b) and immunocytochemistry (Fig. 2, i-n and i'-n').

To determine whether the perinuclear Nrg3 immunostaining in the detergent-permeabilized samples corresponded to the Golgi apparatus, we performed double-labeling immunocytochemistry with serum 6144 and an antibody directed against GM-130, a resident molecule of the cis-Golgi apparatus (Nakamura et al., 1995). As shown in Fig. 3, a-c, anti-Nrg3 and anti-GM-130 showed overlapping immunoreactivity in the perinuclear region of N2a/Nrg3 cells. This overlap was also observed in the Golgi apparatus of cortical neurons expressing endogenous Nrg3 (Fig. 3, d-f). Nrg3 immunostaining of the Golgi apparatus was not detected in the untransfected N2a cells (Fig. 3, a-c, unt (arrow)), indicating that the Nrg3 staining within the Golgi was not due to a cross-reacting antigen also present in the untransfected cells. We also detected co-localization of Nrg3 and GM-130 in detergent-treated P7 rat cortical tissue sections expressing endogenous Nrg3 (Fig. 3, h-j), which was not observed in our secondary-only negative control (Fig. 3k).

These results indicate that Nrg3 is primarily expressed in the plasma membrane and in the Golgi apparatus, not only in Nrg3-transfected cells, but also in primary cortical neurons cultured *in vitro* and in neurons present in cortical tissue sections.

3.3 Expression of Nrg3 in primary cortical neurons and glia *in vitro*.

To identify the cell types expressing Nrg3 in the rat brain, we performed immunocytochemistry on isolated cells from rat E17-E18 cortices and immunohistochemistry on tissue sections using markers to identify different neuronal and glial subtypes. As shown in Fig. 4, Nrg3 immunoreactivity was detected in both the cell bodies and processes of neurons that expressed the neuronal marker microtubule-associated protein 2 (MAP2) (Fig. 4, a-c).

Immunofluorescence staining in P4 tissue sections also shows Nrg3 expression on MAP2 expressing cortical neurons (Fig.4, d-f). Nrg3 was also observed in cells expressing the enzyme glutamic acid decarboxylase (GAD-65), a marker of inhibitory GABAergic interneurons (Fig. 4, g-l) (Benson, Watkins, Steward, & Banker, 1994) both in neuronal cultures (Fig. 4, g-i) and P4 tissue sections (Fig. 4, j-l). This is of interest since GABAergic interneurons express the Nrg3 receptor ErbB4 (Vullhorst et al., 2009; Yau, Wang, Lai, & Liu, 2003). As ErbB4 is preferentially expressed in the parvalbumin-positive subset of cortical interneurons, we performed immunofluorescence staining in P7 tissue sections and identified Nrg3 in parvalbumin-expressing neurons (Fig. 4, m-o). The Nrg3 immunostaining was observed throughout the dendritic compartment as well as in the soma of parvalbumin positive interneurons. In the presence of detergent, the Nrg3 cell surface staining was reduced as observed in cultured cells (Fig. 2).

We also examined the expression of Nrg3 in glial cells (Fig. 5) present in dissociated cortical cultures (Fig. 5, a-c and g-i) and in sections of P3 and P7 cerebral cortices-(Fig. 5, d-f and j-l respectively). To determine whether Nrg3 was expressed in astrocytes and oligodendrocytes, we performed immunocytochemistry using an antibody against the glial fibrillary acidic protein (GFAP) (Fig. 5, a-f) and O4 (Fig. 5, g-i), a marker of oligodendrocytic precursors. We used the myelin enzyme 2',3'-cyclic nucleotide 3'-phosphodiesterase (CNPase) to identify oligodendrocytes in cortical tissue sections (Fig. 5, j-l). For both the GFAP (Fig. 5, a-c) and O4-positive cells (Fig. 5, g-i), Nrg3 staining was primarily detected in the perinuclear region consistent with its potential localization to the Golgi apparatus. We observed very low to background levels of Nrg3 staining at the cell surface and also in the cytoplasm of both cell types. These findings were confirmed in tissue sections, with Nrg3 staining only overlapping that of-GFAP (Fig. 5, d-f) and CNPase (Fig. 5, j-l) at the perinuclear region. These observations suggest that the location of Nrg3 in glia may be restricted to the Golgi apparatus, a finding that differs from that in neurons where Nrg3 is present in the soma as well as in the processes.

3.4 Overall expression of Nrg3 mRNA in the rat CNS.

To characterize the spatio-temporal expression of Nrg3 in the rat CNS, we performed immunohistochemistry and *in situ* hybridization studies in tissues derived from rats ranging in age from E19 to P20. We focused on late embryonic and early postnatal stages given the extensive developmental changes that take place during this period.

In sagittal sections from E19 rat embryos (Fig. 6j) we observed high levels of Nrg3 mRNA hybridization in the developing cortical plate (CxP) and also low but detectable levels of hybridization in the ventricular zone (VZ) and subventricular zones (SVZ) (also see Fig. 7a). We also observed hybridization in the developing hippocampal formation (Hi) and detected high levels of Nrg3 hybridization within the developing thalamic region (Th). In contrast, very low to background levels of Nrg3 hybridization were detected in the developing striatum (CPu). More posteriorly, we observed generalized Nrg3 mRNA hybridization in the mesencephalon, with extensive hybridization observed in the dorsal structures such as the superior and inferior colliculi (SC and IC respectively), and also in the more ventral structures. We also observed generalized hybridization throughout the hindbrain with a prominent signal in the pontine nucleus (Pn). At E19, Nrg3 hybridization in the cerebellum (Cb) was still sparse, in contrast to later developmental stages as shown in Fig. 6h and k, in Fig. 8 and Fig. 10i.

We also conducted *in situ* hybridization on coronal sections of P7 rat brain (Fig. 6, a-i). Within the olfactory bulb Nrg3 was detected in the anterior olfactory nucleus (AON) and the mitral (Mi) and glomerular cell layers (GI) (Fig. 6a). Low levels of Nrg3 hybridization were detected in the internal granule layer (IGr). Nrg3 was also expressed at high levels throughout the frontal (Fr), orbital (Orb), cingulate (Cg), and piriform cortex (Pir) (Fig. 6, b and c). The widespread high levels of hybridization throughout all cortical layers were maintained in both anterior and posterior regions. As shown in Fig. 6d, the caudate/putamen (CPu) showed overall very low levels of hybridization with some areas showing higher mRNA levels resulting in an

overall patched appearance (Fig. 6d and Fig. 10g). High levels of Nrg3 mRNA were also observed in the tenia tecta (TT) and the lateral septal nucleus (LSN) (Fig. 6d). In addition, Nrg3 mRNA was observed at high levels in the thalamus including the medial-dorsal (MD) and ventral thalamic nuclei (VP) (Fig. 6e). In the hippocampal formation, Nrg3 mRNA was expressed in the CA1-CA3 regions with lower levels of hybridization detected in the dentate gyrus (DG) at this developmental stage (Fig. 6, e-g, Fig. 9 and Fig. 10h). Nrg3 mRNA was detected in the medial habenula (Mhb), the dorsal endopiriform nucleus (DEN), the posterolateral cortical amygdaloid nucleus (PCLo) (Fig. 6e), and the basolateral (BLA) and basomedial (BMA) amygdala (Fig. 6f). The ventral cochlear nucleus (VCA), as well as the superior (SC) and inferior colliculi (IC), also showed high levels of Nrg3 mRNA (Fig. 6, g and h). As observed at E19, there was particularly high expression of Nrg3 mRNA in the pontine nucleus (Pn) (Fig. 6i).

In situ hybridization of Nrg3 mRNA in sagittal sections of P20 rat brains showed that Nrg3 mRNA levels remained high and widely distributed throughout the CNS (Fig. 6k). As observed in earlier stages of development, high levels of Nrg3 mRNA hybridization were observed throughout the cerebral cortex (Cx) as well as the anterior olfactory nucleus (AON) in the olfactory bulb (Fig. 6k). The striatum (CPu) showed higher levels of Nrg3 hybridization than at earlier stages. At this stage, the hippocampal formation is fully developed with Nrg3 mRNA present in areas CA1-CA3 and also within the dentate gyrus (DG). Nrg3 expression remained high within the thalamic region, as observed by the strong hybridization signal detected within the ventrolateral (VL), ventral posteromedial (VPM), and lateral posterior (LP) nuclei of the thalamus. In the cerebellum, Nrg3 mRNA was detected in the Purkinje neurons (PCL), the granule cell layer (GL), and the cerebellar nuclei (CerN) (Fig. 6k and Fig. 8). In the hindbrain, a signal was clearly distinguished in the facial nucleus (Fig. 6k labeled "7"). At all ages examined we observed very low to background levels of Nrg3 hybridization within the white matter as illustrated by the low Nrg3 mRNA hybridization signal in the corpus callosum (cc) (Fig. 6d and k), the internal capsule (ic) (Fig. 6k), and cerebellar white matter (wm) (Fig. 6h and k).

3.5 Developmental localization of Nrg3 in the cortex

To examine the developmental expression of Nrg3 in the cerebral cortex, we performed *in situ* hybridization as well as immunofluorescent staining. As shown in Fig. 7a, *in situ* hybridization of Nrg3 at E17 showed strong hybridization throughout the cortical plate (CxP) both anteriorly and posteriorly (Fig. 7a). Nrg3 mRNA was also detected in the ventricular and subventricular zones (VZ and SVZ) (Fig. 7a). These findings were consistent with those observed by immunohistochemical staining (Fig. 7b) showing clear anti-Nrg3 staining in the cortical plate (CxP), and lighter staining in the intermediate zone (IZ). We also observed Nrg3 expression along the ventricular lining (VZ) (Fig. 7, b and c). At this stage (E17) Nrg3 staining was observed in the soma and neuronal processes extending radially within the cortical plate (see arrows in Fig. 7d). Within the upper cortical layers there was extensive co-localization of Nrg3 with the neuronal marker MAP2 (Fig. 7, e-g). The Nrg3-expressing cells were not restricted to the cortical plate (CxP) as cells in the subplate (SP) and intermediate zones (IZ) also expressed Nrg3 (Fig. 7e). At P3, a developmental stage in which the cortex is undergoing dynamic changes in connectivity and cellular differentiation, we observed continued expression of Nrg3 mRNA and protein throughout all cortical layers (Fig. 7, h and i) as was also seen at P7 (Fig. 7, j and k). As shown in the sagittal sections of the P20 brain (Fig. 6k), the expression of Nrg3 mRNA remained elevated at late postnatal stages throughout the brain.

3.6 Developmental localization of Nrg3 in the cerebellum.

We analyzed the expression of Nrg3 in the cerebellum at three developmental stages that represent distinct stages of cerebellar maturation P3, P7, and P20. Unlike the cerebral cortex and many other brain structures, the development of the cerebellum occurs largely in the postnatal period (Caceres, Banker, Steward, Binder, & Payne, 1984). At P3, the expression of Nrg3 mRNA in the external granule cell layer (EGL) is at background levels (Fig. 8a). However,

a low level of Nrg3 expression was observed in the internal granule cell layer (IGL). At this stage, the cells in the EGL are actively proliferating and the resulting neuroblasts are beginning to migrate internally past the Purkinje (PC) neurons to form the internal granule cell layer (IGL) (Fig. 8a). At P7, when the generation of granule neurons in the EGL is at its peak, we observed low levels of Nrg3 expression in the EGL but much higher levels of Nrg3 mRNA in the granule neurons that had migrated into the IGL (Fig. 8b). We also compared the localization of Nrg3 mRNA to that of Nrg1 type III mRNA at P7 (Fig. 8c). Unlike Nrg3 mRNA, Nrg1 type III shows low levels of expression in the IGL and EGL but high levels of hybridization in large neurons consistent with its localization to Golgi neurons. These differences suggest distinct biological functions for Nrg3 and Nrg1 type III in the cerebellum at this stage. It was difficult to determine from these *in situ* hybridization experiments whether the PC neurons expressed Nrg3 mRNA. To address this question we performed immunofluorescence staining (Fig. 8, e-g) and determined that Nrg3 was expressed in PC neurons as demonstrated by co-localization of Nrg3 with calbindin (Fig. 8g), a Ca^{2+} -binding protein expressed by these neurons. We further analyzed whether Nrg3 was expressed in astrocytes and Bergmann glia (BG) by using GFAP as a marker. Consistent with our observations in cortical cultures and cortical sections, only low to background levels of Nrg3 were observed in glia (Fig. 8h and Fig. 5, a-f). We also analyzed the distribution of Nrg3 at P20 (Fig. 8d), a stage in which the migration of the granule neurons into the IGL is complete. At this stage, the expression of Nrg3 mRNA in the Purkinje cell layer (PCL) was evident by *in situ* hybridization with lower but clearly detectable levels in the IGL. In contrast, the molecular layer (ML) at this stage, which is composed mainly of granule neuron axons and the dendritic arbors of PC neurons, showed low to background levels of Nrg3 mRNA (Fig. 8d).

3.7 Developmental localization of Nrg3 in the hippocampus.

We examined the developmental expression of Nrg3 in the hippocampus. As shown in Figure 9, *in situ* hybridization showed that Nrg3 mRNA was present throughout areas CA1-3 at the three developmental stages examined P3, P7, and P25 (Fig. 9, a-c respectively). The dentate gyrus (DG), unlike areas CA1-3, is primarily formed during the postnatal period and the Nrg3 mRNA hybridization levels closely reflect this developmental pattern of maturation. At P3 (Fig. 9a), low levels of hybridization were observed in the DG anlagen, progressively increasing through P25 (Fig. 9c). At P25, the Nrg3 mRNA hybridization signal in the DG matches or exceeds that observed in areas CA1-3 (Fig. 9c). Consistent with the mRNA localization, immunofluorescence also showed Nrg3 labelling of cell processes and the soma of neurons in these areas (CA1 shown in Fig. 9, d and e; the dentate gyrus shown in Fig. 9, f and g).

3.8 Comparison of the localization of Nrg1 type III, Nrg2, and Nrg3 mRNAs in P7 rat brain.

To identify areas in which the Nrgs, including Nrg3, could have unique or shared functions, we compared the distribution of Nrg to that of Nrg1 type III and Nrg2 mRNAs in P7 rat brains by *in situ* hybridization. Nrg3 showed high levels of hybridization throughout all cortical layers, as previously described (Bartolini et al., 2017; Longart et al., 2004) (Figs. 6 and 7 and in Fig. 10, g and h). Nrg2 mRNA hybridization was detected throughout the cerebral cortex with the highest levels concentrated in the upper cortical layers (Fig. 10, d and e). Nrg1 type III mRNA hybridization was also observed throughout the cerebral cortex, with the highest levels detected in the upper cortical layers. It was particularly prominent in layer V (Fig. 10, a and b). In the hippocampus, although all three Nrgs were present throughout areas CA1-3, they exhibited clear differences. Nrg1 type III mRNA had a more prominent expression in area CA3 than in CA1 or the DG (Fig. 10b), while both Nrg2 and Nrg3 seemed evenly distributed among the CA1-3 regions at this stage (Fig. 10, e and h respectively). In the DG, the hybridization levels of Nrg2 were comparable to those in areas CA1-CA3 while those of Nrg1 type III and Nrg3 were less intense than those detected at CA1-3 at this developmental stage (Fig. 10, e, b

and h respectively). Nrg3 and Nrg2 mRNAs were widely distributed throughout the thalamic region (Fig. 10, e and h) while NRG1 type III showed a more selective expression in the medial habenula (Mhb) and the reticular nuclei of the thalamus (Rt) (Fig. 10b). As previously described, only background levels of Nrg3 mRNA hybridization were observed in the striatum (CPu), however higher levels of Nrg2 were observed in this region (Fig. 10, g and d respectively and Fig. 6d). Nrg1 type III also showed clear hybridization in the arcuate nucleus (Arc) and the paraventricular nucleus of the thalamus (Pa) (Fig. 10b), unlike Nrg2 and Nrg3. At P7, in the cerebellum, Nrg2 and Nrg3 (Fig. 10, f and i) were expressed in the internal granule cell layer (IGL) while Nrg1 type III expression was restricted to the Golgi neurons and possibly Bergmann glia, as previously described (Fig. 10c and Fig. 8c). Immunofluorescent staining with an antibody specific to Nrg1 type III is required to unambiguously determine Nrg 1 type III expression in these glia. Overall, Nrg2 and Nrg3 were expressed in a greater number of brain regions than Nrg1 type III, whose expression is more restricted.

4 DISCUSSION

The neuregulins (Nrgs) and their receptors the ErbBs play diverse and important roles in the peripheral (PNS) and central (CNS) nervous system. We have characterized the developmental expression and localization of Nrg3 in the rat CNS in order to gain insight into its function. Previous studies have suggested that Nrg3 is more widely expressed than the other Nrgs. However, as these studies have been limited in scope, we sought to provide a more extensive description of the localization of Nrg3 by *in situ* hybridization and immunohistological analyses.

Our study provides additional support for the widespread expression of Nrg3, a pattern that is more extensive than that observed for either Nrg1 (M. S. Chen et al., 1994; Corfas, Rosen, Aratake, Krauss, & Fischbach, 1995; X. Liu et al., 2011; Marchionni et al., 1993; Meyer

et al., 1997; Pinkas-Kramarski et al., 1994) or Nrg2 (Longart et al., 2004). Regions with particularly notable levels of expression include the cortical plate, the mature cerebral cortex, hippocampus, thalamus, cerebellum, and the brain stem. In contrast to the other Nrgs, Nrg3 remains high at later stages of development suggesting that it plays a role in the mature brain (Fig. 10). At the subcellular level, Nrg3 was observed in the plasma membrane of the neuronal cell body and dendritic compartment, with very prominent localization to the Golgi apparatus. Its expression in neurons was more prominent than that observed in glial cells. These immunocytochemical observations are consistent with those reported by Wang et al (Y. N. Wang et al., 2018) that showed expression of Nrg3 in lysates of cultured neurons but not in those of astrocytes. The expression of Nrg1 is not limited to neurons and there are multiple reports showing Nrg1 in brain astrocytes (Kerber, Streif, Schwaiger, Kreutzberg, & Hager, 2003; X. Liu et al., 2011; Pinkas-Kramarski et al., 1994; Tokita et al., 2001).

The expression of Nrg3 was not restricted to glutamatergic neurons but was also identified in GABAergic neurons in culture and in tissue sections. In addition to its expression in GABAergic Purkinje neurons, Nrg3 was detected in parvalbumin-positive neurons, a finding consistent with single cell transcriptome studies (Tasic et al., 2016). We also detected the presence of Nrg3 in dendrites, a compartment critical for integrating synaptic inputs. Two recent observations have shown that Nrg3 can also function within the axonal compartment. In one study, overexpression of Nrg3 resulted in its accumulation in axonal varicosities (Vullhorst et al., 2017). Using biochemical approaches, a separate study showed that Nrg3 is present in post-synaptic density fractions and that it associates with components of the pre-but not post-synaptic terminals, specifically with the SNARE complex (Y. N. Wang et al., 2018). As a consequence of this association, Nrg3 influences synaptic function. The deletion of Nrg3 in *GFAP-Nrg3^{fl/fl}* mice increased glutamatergic transmission whereas increased levels of Nrg3 led to a reduction in transmission. Intriguingly, these roles for Nrg3 appear to be independent of ErbB4 (Y. N. Wang et al., 2018).

One of the most significant observations to emerge from this study is that in addition to its plasma membrane expression, Nrg3 is prominently expressed in the Golgi apparatus. Even in glial cells that only exhibit low levels of expression, Nrg3 was detected in a perinuclear compartment consistent with localization to the Golgi apparatus. Like other secreted and transmembrane proteins, this localization is likely to reflect its transit from the endoplasmic reticulum to the Golgi. In addition to trafficking, the Golgi is also important for post-translational modifications, such as glycosylation and proteolytic cleavage. Like Nrg1 type III, Nrg3 has an amino-terminal transmembrane (TM_N) domain and a carboxyl-terminal transmembrane (TM_C) domain (Zhang et al., 1997). Recent work has shown that the protease, BACE1, can proteolytically cleave Nrg3 at a site between the TM_C and the EGF-like domain (Vullhorst et al., 2017). This yields a transmembrane form of Nrg3 that remains tethered to the membrane by its TM_N domain, with its N-terminus located inside of the cell and with its EGF-like domain displayed outside of the cell. This cleavage event was thought to occur in the Golgi as mutations that prevented the proteolytic processing resulted in increased levels of Nrg3 in this compartment. Similar mutations in Nrg1 type III did not lead to accumulation in the Golgi, but instead resulted in its dispersion throughout the cell. These findings suggested that the role of the Golgi in Nrg3 post-translational processing may differ from that of Nrg1 type III (Vullhorst et al., 2017). Proteolytic processing in the Golgi is not limited to Nrg3 and Nrg1 type III as it has also been reported for other Nrg1 subtypes (Ben Halima et al., 2016; Fleck et al., 2013; Loeb, Susanto, & Fischbach, 1998; Montero et al., 2007; J. Y. Wang, Miller, & Falls, 2001; Yokozeki et al., 2007).

One of the possible explanations for the prevalence of Nrg3 in the Golgi apparatus is that Nrg3 undergoes O-linked glycosylation. Unlike N-linked glycosylation that occurs co-translationally in the endoplasmic reticulum with subsequent remodeling in the Golgi, the enzymes that perform O-linked glycosylation are localized within the Golgi (Hang & Bertozzi, 2005; Hanisch, 2001; Kudelka, Ju, Heimburg-Molinaro, & Cummings, 2015). In this study, we

demonstrated that treatment of P25 cerebral cortical extracts with a combination of neuraminidase and O-glycanase resulted in a substantial reduction in its molecular weight. A more limited reduction was detected in Nrg3 from E18 cortex. These data indicate a developmental shift in the sugar content for Nrg3. O-glycanase requires the removal of peripheral branches before it can cleave the core GalNAc/GlcNAc disaccharide linking the sugar chains to the serine/threonine residues on the core protein (Hanisch, 2001). Consistent with this fact, neuraminidase treatment alone resulted in a molecular weight reduction of Nrg3, which was further enhanced by co-incubation with O-glycanase. In contrast, O-glycanase by itself did not result in a significant reduction in Nrg3 molecular weight. PNGase did not reduce the molecular weight of Nrg3, in agreement with the prediction by Zhang et al (Zhang et al., 1997) that Nrg3 lacks potential N-linked glycosylation sites. This same group described a region near the amino-terminal end of Nrg3, corresponding to a sequence rich in serines and threonines such as that found in mucins (mucin-like). These stretches concentrate GalNAc-based glycans since they can be subject to serial O-linked glycosylation (Hang & Bertozzi, 2005). An alternatively spliced form of human NRG3 appears to contain β -N-acetyl galactosamine based on its ability to interact with soybean agglutinin, which preferentially binds to Gal NAc-containing sugars (Carteron et al., 2006). This human NRG3 variant lacks the mucin-like stretch, suggesting that Nrg3 can undergo O-linked glycosylation at sites other than within the mucin-like region. It will be important to identify what residues are glycosylated in Nrg3 as well as the developmental time course of these modifications. Other Nrgs have been shown to be both N- and O-linked glycosylated (Cabedo, Carteron, & Ferrer-Montiel, 2004; Loeb et al., 1998; Lu et al., 1995; Peles et al., 1992; Shamir & Buonanno, 2010; J. Y. Wang et al., 2001; Wen et al., 1994). The developmental differences in Nrg3 glycosylation likely influence its functional properties. O-linked glycosylation has been previously shown to modify protein structure, affect the availability of proteolytic cleavage sites, modulate protein-protein interactions, and alter protein compartmentalization and trafficking.

Nrg3 is highly abundant and widely expressed in the cerebral cortex from early stages of development into adulthood as shown in Figure 7 and as described in previous studies (Bartolini et al., 2017; Longart et al., 2004; Zhang et al., 1997). This distribution differs from that of Nrg2 and Nrg1 type III (Fig. 10), as these Nrgs are expressed more prominently in the upper cortical layers than in the lower layers (also see (M. S. Chen et al., 1994; Corfas et al., 1995; Longart et al., 2004; Meyer et al., 1997)). In layer V, the expression of Nrg1 type III is particularly notable. In contrast to previous studies, we show for the first time, by both *in situ* hybridization and immunohistochemistry, that Nrg3 is expressed in cells lining the ventricular surface. The localization of Nrg3 in the ventricular zone (VZ) suggests potential roles in the proliferation of neuronal and glial precursors, differentiation (such as radial glial differentiation), and in neuroblast migration. Previous studies have identified the presence of Nrgs in neuroblasts. Nrgs1 and 2 have been detected in neuroblasts present in the postnatal anterior subventricular zone (SVZ) (Ghashghaei et al., 2006). In addition, Nrg1 has been shown to induce the proliferation of neural progenitor cells derived from E11 mouse cortex (Y. Liu, Ford, Mann, & Fischbach, 2005). Our observations showing the presence of Nrg3 in the VZ raises the possibility that Nrg3 could play a proliferative role in cells expressing ErbB4 in the VZ.

The earliest description of Nrg3 expression in cortical development at E12.5 (Assimacopoulos et al., 2003) supports the hypothesis of a potential role of Nrg3 acting by itself or synergistically with Nrg1 in the establishment of radial glia. At this stage Nrg3, Nrg1, and TGF α are expressed in the anti-hem, an area flanking the lateral neuroepithelium that gives rise to the cerebral cortex. Another structure, the hem, which acts as an organizing center, also flanks the neuroepithelium but on its medial aspect (Subramanian, Remedios, Shetty, & Tole, 2009). As elimination of the anti-hem results in loss of the radial glial palisade at the pallial-subpallial boundary (Kim, Anderson, Rubenstein, Lowenstein, & Pleasure, 2001; Stenman, Yu, Evans, & Campbell, 2003; Yun, Potter, & Rubenstein, 2001), it has been proposed that expression of Nrg1 in the anti-hem contributes to the formation and maintenance of this radial

glial palisade at this early developmental stage (Subramanian et al., 2009). The contribution of each Nrg (1 and 3) at the anti-hem in the establishment and maintenance of the radial glia palisade at this early age remains to be determined. Nrg1/ErbB2/4 signaling has been implicated in the establishment and maintenance of the radial glia phenotype in the cortex (Anton, Marchionni, Lee, & Rakic, 1997; Schmid et al., 2003) and the cerebellum (Rio, Rieff, Qi, Khurana, & Corfas, 1997), however the role of the ErbB2 and ErbB4 in this process has been challenged (see Barros et al (Barros et al., 2009)).

A newly identified role for Nrg3 is in the guidance of migrating interneurons in the developing cortex. These cells express ErbB4 and it has been previously shown that they migrate tangentially from the ganglionic eminences into the cortex. This process is influenced by distinct isoforms of Nrg1, which serve as both short- and long-range attractants (Bartolini et al., 2017; Flames et al., 2004). When the migrating cells have completed their tangential migration, Nrg3 serves as an important factor that helps to guide GABAergic interneurons as they migrate radially into their appropriate final laminar destination in the cortex (Bartolini et al., 2017).

In the hippocampus, Nrg3 is the most abundantly expressed Nrg. We observed Nrg3 in areas CA1-CA3 and in the granule neurons of the dentate gyrus (DG). Expression in the hippocampal formation was high throughout development and remained high at P25, suggesting that Nrg3 may play roles both during development and in the mature hippocampus. In contrast, the developmental expression of both Nrg1 type III and Nrg2 in CA1-3 differs significantly from that of Nrg3. Previously, Longart et al (Longart et al., 2004) reported that the expression of Nrg2 in CA1-CA3, is transient showing a bell-shaped expression pattern. It increases from P0 to P7 and then decreases significantly by P25 (Longart et al., 2004). In contrast, Nrg1 type III shows its highest expression levels in the CA3 region with only low to background levels in the CA1 at P7. Thus at the mRNA level, it appears that Nrg3 is the primary Nrg expressed in CA1, while in CA3 it is expressed along with Nrg1 type III. As the DG matures, its granule neurons

express significant levels of both Nrg3 and Nrg2 at late postnatal stages, while Nrg1 type III levels are much lower. There have been multiple studies highlighting the role of Nrgs in hippocampal function and plasticity (Buonanno, 2010; Mei & Nave, 2014; Mei & Xiong, 2008) and it will be interesting to determine if Nrg3 plays a similar role in these processes.

In the cerebellum, Nrg3 was expressed in the granule cell layer and in Purkinje neurons in a pattern resembling that of Nrg2 (Longart et al., 2004). The expression of Nrg1 in the cerebellum is isoform dependent with types I and II reported in cerebellar granule and Purkinje neurons (Corfas et al., 1995; Kerber et al., 2003; Rio et al., 1997). Nrg1 type III differs from these isoforms and is detected in Golgi type I neurons (see Fig. 8), as has been previously reported (Corfas et al., 1995; Longart et al., 2004). In addition, we also observed detectable hybridization of Nrg1 type III in cells near the border of the molecular layer. Antibody staining will be required to ascertain the identity of these cells. In view of the aforementioned role of Nrg3 in cortical interneuronal migration (Bartolini et al., 2017), it will be of interest to determine whether it also plays a role in the migration of cerebellar granule neurons. Nrg1 has been previously shown to promote granule cell migration via an interaction with ErbB4, which is expressed on Bergmann glial fibers (Rio et al., 1997). Although the expression of ErbB4 by cerebellar granule cells has been controversial (Bean et al., 2014), our studies (not shown) and those of others (Elenius et al., 1997; Pinkas-Kramarski et al., 1997), have provided evidence supporting its expression in granule neurons both in tissue sections and *in vitro* (Rieff et al., 1999; Rio et al., 1997; Xie, Padival, & Siegel, 2007). Perez-Garcia (Perez-Garcia, 2015) and our own unpublished work, have observed ectopic clusters of granule neurons at the surface of the EGL in ErbB4 deficient mice. These observations also support a role for ErbB4 in cerebellar granule cell migration. Nrg1/ErbB4 signaling has also been shown to promote an increase in dendritic outgrowth of cerebellar granule neurons *in vivo* (Rieff & Corfas, 2006; Rieff et al., 1999). In view of the role of Nrg3 in GABAergic cell migration in the cortex (Bartolini et al.,

2017), it is possible that it also plays a developmental role in the migration of cerebellar granule neurons.

Although they have partially overlapping patterns of expression, each of the Nrgs is expressed in a distinct manner. In addition to the brain regions discussed in the preceding paragraphs, Nrg3 is broadly expressed in a number of thalamic and hypothalamic nuclei and throughout the brain stem, a pattern distinct from the other Nrgs. Furthermore, the hybridization levels detected for Nrg3 were significantly higher than the other Nrgs. These observations suggest that the Nrgs serve different functions in the nervous system. Nrg1 plays an essential role in peripheral myelination, a role not shared by either Nrg2 or Nrg3 (Birchmeier & Bennett, 2016; Mei & Nave, 2014). In neurons in the CNS, ErbB4 is the most readily detected ErbB and it has largely been assumed that ErbB4-expressing neurons are the likely target of activation by Nrgs 1, 2, and 3. A recent report, however, has revealed that Nrg3 can regulate glutamatergic neurotransmission in an ErbB4-independent manner (Y. N. Wang et al., 2018). This finding leads to the speculation that other Nrgs may have functions that do not require activation of an ErbB receptor. Indeed, this has been reported for Nrg2, which has been shown to regulate GABAR alpha 1 expression. In this case, ErbB4 is required but it functions in a manner that does not require its tyrosine kinase activity (Mitchell et al., 2013). The identification of an ErbB4-independent role for Nrg3 provides an additional layer of complexity as one can no longer simply compare its expression profile to the known sites of ErbB expression in order to identify potential targets of Nrg3 activity.

In summary, Nrg3 is the most abundantly expressed Nrg in the brain and an improved understanding of its site of expression should facilitate our ability to identify novel functional roles for this molecule.

CONFLICT OF INTEREST.

The authors declare no competing interests, financial or other.

AUTHOR CONTRIBUTIONS

Afrida Rahman, Janet Weber, Edward Labin and Anne L. Prieto performed the experiments and collected the data, and Afrida Rahman, Cary Lai, and Anne L. Prieto conceived the experiments, analyzed the data, and wrote the manuscript.

REFERENCES

- Aghajanian, G. K., & Bloom, F. E. (1967). The formation of synaptic junctions in developing rat brain: a quantitative electron microscopic study. *Brain Res*, *6*(4), 716-727.
- Anton, E. S., Ghashghaei, H. T., Weber, J. L., McCann, C., Fischer, T. M., Cheung, I. D., . . . Lai, C. (2004). Receptor tyrosine kinase ErbB4 modulates neuroblast migration and placement in the adult forebrain. *Nat Neurosci*, *7*(12), 1319-1328.
- Anton, E. S., Marchionni, M. A., Lee, K. F., & Rakic, P. (1997). Role of GGF/neuregulin signaling in interactions between migrating neurons and radial glia in the developing cerebral cortex. *Development*, *124*(18), 3501-3510.
- Assimacopoulos, S., Grove, E. A., & Ragsdale, C. W. (2003). Identification of a Pax6-dependent epidermal growth factor family signaling source at the lateral edge of the embryonic cerebral cortex. *J Neurosci*, *23*(16), 6399-6403.
- Avramopoulos, D. (2018). Neuregulin 3 and its roles in schizophrenia risk and presentation. *Am J Med Genet B Neuropsychiatr Genet*, *177*(2), 257-266. doi:10.1002/ajmg.b.32552
- Bai, Y., Li, J., Fang, B., Edwards, A., Zhang, G., Bui, M., . . . Haura, E. B. Phosphoproteomics identifies driver tyrosine kinases in sarcoma cell lines and tumors. *Cancer Res*, *72*(10), 2501-2511. doi:0008-5472.CAN-11-3015 [pii] 10.1158/0008-5472.CAN-11-3015
- Barros, C. S., Calabrese, B., Chamero, P., Roberts, A. J., Korzus, E., Lloyd, K., . . . Muller, U. (2009). Impaired maturation of dendritic spines without disorganization of cortical cell layers in mice lacking NRG1/ErbB signaling in the central nervous system. *Proc Natl Acad Sci U S A*, *106*(11), 4507-4512. doi:10.1073/pnas.0900355106
- Bartolini, G., Sanchez-Alcaniz, J. A., Osorio, C., Valiente, M., Garcia-Frigola, C., & Marin, O. (2017). Neuregulin 3 Mediates Cortical Plate Invasion and Laminar Allocation of GABAergic Interneurons. *Cell Rep*, *18*(5), 1157-1170. doi:10.1016/j.celrep.2016.12.089
- Bean, J. C., Lin, T. W., Sathyamurthy, A., Liu, F., Yin, D. M., Xiong, W. C., & Mei, L. (2014). Genetic labeling reveals novel cellular targets of schizophrenia susceptibility gene: distribution of GABA and non-GABA ErbB4-positive cells in adult mouse brain. *J Neurosci*, *34*(40), 13549-13566. doi:10.1523/JNEUROSCI.2021-14.2014

- Ben Halima, S., Mishra, S., Raja, K. M. P., Willem, M., Baici, A., Simons, K., . . . Rajendran, L. (2016). Specific Inhibition of beta-Secretase Processing of the Alzheimer Disease Amyloid Precursor Protein. *Cell Rep*, *14*(9), 2127-2141. doi:10.1016/j.celrep.2016.01.076
- Benson, D. L., Watkins, F. H., Steward, O., & Banker, G. (1994). Characterization of GABAergic neurons in hippocampal cell cultures. *J Neurocytol*, *23*(5), 279-295.
- Birchmeier, C., & Bennett, D. L. (2016). Neuregulin/ErbB Signaling in Developmental Myelin Formation and Nerve Repair. *Curr Top Dev Biol*, *116*, 45-64. doi:10.1016/bs.ctdb.2015.11.009
- Buonanno, A. (2010). The neuregulin signaling pathway and schizophrenia: from genes to synapses and neural circuits. *Brain Res Bull*, *83*(3-4), 122-131. doi:S0361-9230(10)00169-3 [pii] 10.1016/j.brainresbull.2010.07.012
- Cabedo, H., Carteron, C., & Ferrer-Montiel, A. (2004). Oligomerization of the sensory and motor neuron-derived factor prevents protein O-glycosylation. *J Biol Chem*, *279*(32), 33623-33629. doi:10.1074/jbc.M401962200
- Caceres, A., Banker, G., Steward, O., Binder, L., & Payne, M. (1984). MAP2 is localized to the dendrites of hippocampal neurons which develop in culture. *Brain Res*, *315*(2), 314-318.
- Cappellini, M. D., Cohen, A., Piga, A., Bejaoui, M., Perrotta, S., Agaoglu, L., . . . Alberti, D. (2006). A phase 3 study of deferasirox (ICL670), a once-daily oral iron chelator, in patients with beta-thalassemia. *Blood*, *107*(9), 3455-3462. doi:10.1182/blood-2005-08-3430
- Carraway, K. L., 3rd, Weber, J. L., Unger, M. J., Ledesma, J., Yu, N., Gassmann, M., & Lai, C. (1997). Neuregulin-2, a new ligand of ErbB3/ErbB4-receptor tyrosine kinases. *Nature*, *387*(6632), 512-516. doi:10.1038/387512a0
- Carteron, C., Ferrer-Montiel, A., & Cabedo, H. (2006). Characterization of a neural-specific splicing form of the human neuregulin 3 gene involved in oligodendrocyte survival. *J Cell Sci*, *119*(Pt 5), 898-909. doi:10.1242/jcs.02799
- Chen, M. S., Bermingham-McDonogh, O., Danehy, F. T., Jr., Nolan, C., Scherer, S. S., Lucas, J., . . . Marchionni, M. A. (1994). Expression of multiple neuregulin transcripts in postnatal rat brains. *J Comp Neurol*, *349*(3), 389-400.
- Chen, P. L., Avramopoulos, D., Lasseter, V. K., McGrath, J. A., Fallin, M. D., Liang, K. Y., . . . Valle, D. (2009). Fine mapping on chromosome 10q22-q23 implicates Neuregulin 3 in schizophrenia. *Am J Hum Genet*, *84*(1), 21-34. doi:S0002-9297(08)00626-5 [pii] 10.1016/j.ajhg.2008.12.005
- Corfas, G., Rosen, K. M., Aratake, H., Krauss, R., & Fischbach, G. D. (1995). Differential expression of ARIA isoforms in the rat brain. *Neuron*, *14*(1), 103-115.

- Elenius, K., Corfas, G., Paul, S., Choi, C. J., Rio, C., Plowman, G. D., & Klagsbrun, M. (1997). A novel juxtamembrane domain isoform of HER4/ErbB4. Isoform-specific tissue distribution and differential processing in response to phorbol ester. *J Biol Chem*, *272*(42), 26761-26768.
- Falls, D. L. (2003). Neuregulins: functions, forms, and signaling strategies. *Exp Cell Res*, *284*(1), 14-30.
- Falls, D. L., Rosen, K. M., Corfas, G., Lane, W. S., & Fischbach, G. D. (1993). ARIA, a protein that stimulates acetylcholine receptor synthesis, is a member of the neu ligand family. *Cell*, *72*(5), 801-815.
- Flames, N., Long, J. E., Garratt, A. N., Fischer, T. M., Gassmann, M., Birchmeier, C., . . . Marin, O. (2004). Short- and long-range attraction of cortical GABAergic interneurons by neuregulin-1. *Neuron*, *44*(2), 251-261.
- Fleck, D., van Bebber, F., Colombo, A., Galante, C., Schwenk, B. M., Rabe, L., . . . Haass, C. (2013). Dual cleavage of neuregulin 1 type III by BACE1 and ADAM17 liberates its EGF-like domain and allows paracrine signaling. *J Neurosci*, *33*(18), 7856-7869. doi:10.1523/JNEUROSCI.3372-12.2013
- Gao, R., & Penzes, P. (2015). Common mechanisms of excitatory and inhibitory imbalance in schizophrenia and autism spectrum disorders. *Curr Mol Med*, *15*(2), 146-167.
- Ghashghaei, H. T., Weber, J., Pevny, L., Schmid, R., Schwab, M. H., Lloyd, K. C., . . . Anton, E. S. (2006). The role of neuregulin-ErbB4 interactions on the proliferation and organization of cells in the subventricular zone. *Proc Natl Acad Sci U S A*, *103*(6), 1930-1935. doi:10.1073/pnas.0510410103
- Grieco, S. F., Holmes, T. C., & Xu, X. (2018). Neuregulin directed molecular mechanisms of visual cortical plasticity. *J Comp Neurol*. doi:10.1002/cne.24414
- Hang, H. C., & Bertozzi, C. R. (2005). The chemistry and biology of mucin-type O-linked glycosylation. *Bioorg Med Chem*, *13*(17), 5021-5034. doi:10.1016/j.bmc.2005.04.085
- Hanisch, F. G. (2001). O-glycosylation of the mucin type. *Biol Chem*, *382*(2), 143-149. doi:10.1515/BC.2001.022
- Hayes, L. N., Shevelkin, A., Zeledon, M., Steel, G., Chen, P. L., Obie, C., . . . Pletnikov, M. V. (2016). Neuregulin 3 Knockout Mice Exhibit Behaviors Consistent with Psychotic Disorders. *Mol Neuropsychiatry*, *2*(2), 79-87. doi:10.1159/000445836
- Holmes, W. E., Sliwkowski, M. X., Akita, R. W., Henzel, W. J., Lee, J., Park, J. W., . . . et al. (1992). Identification of heregulin, a specific activator of p185erbB2. *Science*, *256*(5060), 1205-1210.
- Kao, W. T., Wang, Y., Kleinman, J. E., Lipska, B. K., Hyde, T. M., Weinberger, D. R., & Law, A. J. (2010). Common genetic variation in Neuregulin 3 (NRG3) influences risk for schizophrenia and impacts NRG3 expression in human brain. *Proc Natl Acad Sci U S A*, *107*(35), 15619-15624. doi:1005410107 [pii] 10.1073/pnas.1005410107

- Kerber, G., Streif, R., Schwaiger, F. W., Kreutzberg, G. W., & Hager, G. (2003). Neuregulin-1 isoforms are differentially expressed in the intact and regenerating adult rat nervous system. *J Mol Neurosci*, *21*(2), 149-165. doi:10.1385/JMN:21:2:149
- Kim, A. S., Anderson, S. A., Rubenstein, J. L., Lowenstein, D. H., & Pleasure, S. J. (2001). Pax-6 regulates expression of SFRP-2 and Wnt-7b in the developing CNS. *J Neurosci*, *21*(5), RC132.
- Kudelka, M. R., Ju, T., Heimbarg-Molinaro, J., & Cummings, R. D. (2015). Simple sugars to complex disease--mucin-type O-glycans in cancer. *Adv Cancer Res*, *126*, 53-135. doi:10.1016/bs.acr.2014.11.002
- Lee, K. H., Lee, H., Yang, C. H., Ko, J. S., Park, C. H., Woo, R. S., . . . Lee, S. H. (2015). Bidirectional Signaling of Neuregulin-2 Mediates Formation of GABAergic Synapses and Maturation of Glutamatergic Synapses in Newborn Granule Cells of Postnatal Hippocampus. *J Neurosci*, *35*(50), 16479-16493. doi:10.1523/JNEUROSCI.1585-15.2015
- Liu, X., Bates, R., Yin, D. M., Shen, C., Wang, F., Su, N., . . . Mei, L. (2011). Specific regulation of NRG1 isoform expression by neuronal activity. *J Neurosci*, *31*(23), 8491-8501. doi:10.1523/JNEUROSCI.5317-10.2011
- Liu, Y., Ford, B. D., Mann, M. A., & Fischbach, G. D. (2005). Neuregulin-1 increases the proliferation of neuronal progenitors from embryonic neural stem cells. *Dev Biol*, *283*(2), 437-445. doi:10.1016/j.ydbio.2005.04.038
- Loeb, J. A., Susanto, E. T., & Fischbach, G. D. (1998). The neuregulin precursor proARIA is processed to ARIA after expression on the cell surface by a protein kinase C-enhanced mechanism. *Mol Cell Neurosci*, *11*(1-2), 77-91. doi:10.1006/mcne.1998.0676
- Longart, M., Liu, Y., Karavanova, I., & Buonanno, A. (2004). Neuregulin-2 is developmentally regulated and targeted to dendrites of central neurons. *J Comp Neurol*, *472*(2), 156-172. doi:10.1002/cne.20016
- Loos, M., Mueller, T., Gouwenberg, Y., Wijnands, R., van der Loo, R. J., Neuro, B. M. P. C., . . . Spijker, S. (2014). Neuregulin-3 in the mouse medial prefrontal cortex regulates impulsive action. *Biol Psychiatry*, *76*(8), 648-655. doi:10.1016/j.biopsych.2014.02.011
- Lu, H. S., Chang, D., Philo, J. S., Zhang, K., Narhi, L. O., Liu, N., . . . et al. (1995). Studies on the structure and function of glycosylated and nonglycosylated neu differentiation factors. Similarities and differences of the alpha and beta isoforms. *J Biol Chem*, *270*(9), 4784-4791.
- Marchionni, M. A., Goodearl, A. D., Chen, M. S., Bermingham-McDonogh, O., Kirk, C., Hendricks, M., . . . et al. (1993). Glial growth factors are alternatively spliced erbB2 ligands expressed in the nervous system. *Nature*, *362*(6418), 312-318. doi:10.1038/362312a0
- Mei, L., & Nave, K. A. (2014). Neuregulin-ERBB signaling in the nervous system and neuropsychiatric diseases. *Neuron*, *83*(1), 27-49. doi:10.1016/j.neuron.2014.06.007

- Mei, L., & Xiong, W. C. (2008). Neuregulin 1 in neural development, synaptic plasticity and schizophrenia. *Nat Rev Neurosci*, 9(6), 437-452. doi:10.1038/nrn2392
- Meier, S., Strohmaier, J., Breuer, R., Mattheisen, M., Degenhardt, F., Muhleisen, T. W., . . . Wust, S. (2013). Neuregulin 3 is associated with attention deficits in schizophrenia and bipolar disorder. *Int J Neuropsychopharmacol*, 16(3), 549-556. doi:10.1017/S1461145712000697
- Meyer, D., Yamaai, T., Garratt, A., Riethmacher-Sonnenberg, E., Kane, D., Theill, L. E., & Birchmeier, C. (1997). Isoform-specific expression and function of neuregulin. *Development*, 124(18), 3575-3586.
- Mitchell, R. M., Janssen, M. J., Karavanova, I., Vullhorst, D., Furth, K., Makusky, A., . . . Buonanno, A. (2013). ErbB4 reduces synaptic GABAA currents independent of its receptor tyrosine kinase activity. *Proc Natl Acad Sci U S A*, 110(48), 19603-19608. doi:10.1073/pnas.1312791110
- Montero, J. C., Rodriguez-Barrueco, R., Yuste, L., Juanes, P. P., Borges, J., Esparis-Ogando, A., & Pandiella, A. (2007). The extracellular linker of pro-neuregulin-alpha2c is required for efficient sorting and juxtacrine function. *Mol Biol Cell*, 18(2), 380-393. doi:10.1091/mbc.E06-06-0511
- Morar, B., Dragovic, M., Waters, F. A., Chandler, D., Kalaydjieva, L., & Jablensky, A. (2011). Neuregulin 3 (NRG3) as a susceptibility gene in a schizophrenia subtype with florid delusions and relatively spared cognition. *Mol Psychiatry*, 16(8), 860-866. doi:mp201070 [pii] 10.1038/mp.2010.70
- Nakamura, N., Rabouille, C., Watson, R., Nilsson, T., Hui, N., Slusarewicz, P., . . . Warren, G. (1995). Characterization of a cis-Golgi matrix protein, GM130. *J Cell Biol*, 131(6 Pt 2), 1715-1726.
- Paterson, C., & Law, A. J. (2014). Transient overexposure of neuregulin 3 during early postnatal development impacts selective behaviors in adulthood. *PLoS One*, 9(8), e104172. doi:10.1371/journal.pone.0104172
- Paterson, C., Wang, Y., Hyde, T. M., Weinberger, D. R., Kleinman, J. E., & Law, A. J. (2017). Temporal, Diagnostic, and Tissue-Specific Regulation of NRG3 Isoform Expression in Human Brain Development and Affective Disorders. *Am J Psychiatry*, 174(3), 256-265. doi:10.1176/appi.ajp.2016.16060721
- Peles, E., Bacus, S. S., Koski, R. A., Lu, H. S., Wen, D., Ogden, S. G., . . . Yarden, Y. (1992). Isolation of the neu/HER-2 stimulatory ligand: a 44 kd glycoprotein that induces differentiation of mammary tumor cells. *Cell*, 69(1), 205-216.
- Perez-Garcia, C. G. (2015). ErbB4 in Laminated Brain Structures: A Neurodevelopmental Approach to Schizophrenia. *Front Cell Neurosci*, 9, 472. doi:10.3389/fncel.2015.00472

- Pinkas-Kramarski, R., Eilam, R., Alroy, I., Levkowitz, G., Lonai, P., & Yarden, Y. (1997). Differential expression of NDF/neuregulin receptors ErbB-3 and ErbB-4 and involvement in inhibition of neuronal differentiation. *Oncogene*, *15*(23), 2803-2815.
- Pinkas-Kramarski, R., Eilam, R., Spiegler, O., Lavi, S., Liu, N., Chang, D., . . . Yarden, Y. (1994). Brain neurons and glial cells express Neu differentiation factor/hereregulin: a survival factor for astrocytes. *Proc Natl Acad Sci U S A*, *91*(20), 9387-9391.
- Prieto, A. L., O'Dell, S., Varnum, B., & Lai, C. (2007). Localization and signaling of the receptor protein tyrosine kinase Tyro3 in cortical and hippocampal neurons. *Neuroscience*, *150*(2), 319-334. doi:10.1016/j.neuroscience.2007.09.047
- Prieto, A. L., Weber, J. L., & Lai, C. (2000). Expression of the receptor protein-tyrosine kinases Tyro-3, Axl, and Mer in the developing rat central nervous system. *J Comp Neurol*, *425*(2), 295-314.
- Prieto, A. L., Weber, J. L., Tracy, S., Heeb, M. J., & Lai, C. (1999). Gas6, a ligand for the receptor protein-tyrosine kinase Tyro-3, is widely expressed in the central nervous system. *Brain Res*, *816*(2), 646-661.
- Rieff, H. I., & Corfas, G. (2006). ErbB receptor signalling regulates dendrite formation in mouse cerebellar granule cells in vivo. *Eur J Neurosci*, *23*(8), 2225-2229. doi:10.1111/j.1460-9568.2006.04727.x
- Rieff, H. I., Raetzman, L. T., Sapp, D. W., Yeh, H. H., Siegel, R. E., & Corfas, G. (1999). Neuregulin induces GABA(A) receptor subunit expression and neurite outgrowth in cerebellar granule cells. *J Neurosci*, *19*(24), 10757-10766.
- Rio, C., Rieff, H. I., Qi, P., Khurana, T. S., & Corfas, G. (1997). Neuregulin and erbB receptors play a critical role in neuronal migration. *Neuron*, *19*(1), 39-50.
- Schmid, R. S., McGrath, B., Berechid, B. E., Boyles, B., Marchionni, M., Sestan, N., & Anton, E. S. (2003). Neuregulin 1-erbB2 signaling is required for the establishment of radial glia and their transformation into astrocytes in cerebral cortex. *Proc Natl Acad Sci U S A*, *100*(7), 4251-4256.
- Shamir, A., & Buonanno, A. (2010). Molecular and cellular characterization of Neuregulin-1 type IV isoforms. *J Neurochem*, *113*(5), 1163-1176. doi:10.1111/j.1471-4159.2010.06677.x
- Simmons, D. M., Arriza, L. W., & Swanson, L. (1989). A complete protocol for in situ hybridization of messenger RNAs in brain and other tissues with radio-labeled single stranded RNA probes. *Journal of Histotech*, *12*, 169-181.
- Steinthorsdottir, V., Stefansson, H., Ghosh, S., Birgisdottir, B., Bjornsdottir, S., Fasquel, A. C., . . . Gulcher, J. R. (2004). Multiple novel transcription initiation sites for NRG1. *Gene*, *342*(1), 97-105. doi:10.1016/j.gene.2004.07.029
- Stenman, J., Yu, R. T., Evans, R. M., & Campbell, K. (2003). Tlx and Pax6 co-operate genetically to establish the pallio-subpallial boundary in the embryonic mouse telencephalon. *Development*, *130*(6), 1113-1122.

- Subramanian, L., Remedios, R., Shetty, A., & Tole, S. (2009). Signals from the edges: the cortical hem and antihem in telencephalic development. *Semin Cell Dev Biol*, 20(6), 712-718. doi:10.1016/j.semcdb.2009.04.001
- Tasic, B., Menon, V., Nguyen, T. N., Kim, T. K., Jarsky, T., Yao, Z., . . . Zeng, H. (2016). Adult mouse cortical cell taxonomy revealed by single cell transcriptomics. *Nat Neurosci*, 19(2), 335-346. doi:10.1038/nn.4216
- Tokita, Y., Keino, H., Matsui, F., Aono, S., Ishiguro, H., Higashiyama, S., & Oohira, A. (2001). Regulation of neuregulin expression in the injured rat brain and cultured astrocytes. *J Neurosci*, 21(4), 1257-1264.
- Tran, D. T., & Ten Hagen, K. G. (2013). Mucin-type O-glycosylation during development. *J Biol Chem*, 288(10), 6921-6929. doi:10.1074/jbc.R112.418558
- Turner, J. R., Ray, R., Lee, B., Everett, L., Xiang, J., Jepson, C., . . . Blendy, J. A. (2014). Evidence from mouse and man for a role of neuregulin 3 in nicotine dependence. *Mol Psychiatry*, 19(7), 801-810. doi:10.1038/mp.2013.104
- Vullhorst, D., Ahmad, T., Karavanova, I., Keating, C., & Buonanno, A. (2017). Structural Similarities between Neuregulin 1-3 Isoforms Determine Their Subcellular Distribution and Signaling Mode in Central Neurons. *J Neurosci*, 37(21), 5232-5249. doi:10.1523/JNEUROSCI.2630-16.2017
- Vullhorst, D., Mitchell, R. M., Keating, C., Roychowdhury, S., Karavanova, I., Tao-Cheng, J. H., & Buonanno, A. (2015). A negative feedback loop controls NMDA receptor function in cortical interneurons via neuregulin 2/ErbB4 signalling. *Nat Commun*, 6, 7222. doi:10.1038/ncomms8222
- Vullhorst, D., Neddens, J., Karavanova, I., Tricoire, L., Petralia, R. S., McBain, C. J., & Buonanno, A. (2009). Selective expression of ErbB4 in interneurons, but not pyramidal cells, of the rodent hippocampus. *J Neurosci*, 29(39), 12255-12264. doi:10.1523/JNEUROSCI.2454-09.2009
- Wang, J. Y., Miller, S. J., & Falls, D. L. (2001). The N-terminal region of neuregulin isoforms determines the accumulation of cell surface and released neuregulin ectodomain. *J Biol Chem*, 276(4), 2841-2851.
- Wang, K. S., Xu, N., Wang, L., Aragon, L., Ciubuc, R., Arana, T. B., . . . Xu, C. (2014). NRG3 gene is associated with the risk and age at onset of Alzheimer disease. *J Neural Transm (Vienna)*, 121(2), 183-192. doi:10.1007/s00702-013-1091-0
- Wang, Y. N., Figueiredo, D., Sun, X. D., Dong, Z. Q., Chen, W. B., Cui, W. P., . . . Mei, L. (2018). Controlling of glutamate release by neuregulin3 via inhibiting the assembly of the SNARE complex. *Proc Natl Acad Sci U S A*, 115(10), 2508-2513. doi:10.1073/pnas.1716322115
- Wen, D., Peles, E., Cupples, R., Suggs, S. V., Bacus, S. S., Luo, Y., . . . et al. (1992). Neu differentiation factor: a transmembrane glycoprotein containing an EGF domain and an immunoglobulin homology unit. *Cell*, 69(3), 559-572.

- Wen, D., Suggs, S. V., Karunakaran, D., Liu, N., Cupples, R. L., Luo, Y., . . . et al. (1994). Structural and functional aspects of the multiplicity of Neu differentiation factors. *Mol Cell Biol*, *14*(3), 1909-1919.
- Xie, F., Padival, M., & Siegel, R. E. (2007). Association of PSD-95 with ErbB4 facilitates neuregulin signaling in cerebellar granule neurons in culture. *J Neurochem*, *100*(1), 62-72. doi:10.1111/j.1471-4159.2006.04182.x
- Yan, L., Shamir, A., Skirzewski, M., Leiva-Salcedo, E., Kwon, O. B., Karavanova, I., . . . Buonanno, A. (2017). Neuregulin-2 ablation results in dopamine dysregulation and severe behavioral phenotypes relevant to psychiatric disorders. *Mol Psychiatry*. doi:10.1038/mp.2017.22
- Yau, H. J., Wang, H. F., Lai, C., & Liu, F. C. (2003). Neural development of the neuregulin receptor ErbB4 in the cerebral cortex and the hippocampus: preferential expression by interneurons tangentially migrating from the ganglionic eminences. *Cereb Cortex*, *13*(3), 252-264.
- Yokozeki, T., Wakatsuki, S., Hatsuzawa, K., Black, R. A., Wada, I., & Sehara-Fujisawa, A. (2007). Meltrin beta (ADAM19) mediates ectodomain shedding of Neuregulin beta1 in the Golgi apparatus: fluorescence correlation spectroscopic observation of the dynamics of ectodomain shedding in living cells. *Genes Cells*, *12*(3), 329-343. doi:10.1111/j.1365-2443.2007.01060.x
- Yun, K., Potter, S., & Rubenstein, J. L. (2001). Gsh2 and Pax6 play complementary roles in dorsoventral patterning of the mammalian telencephalon. *Development*, *128*(2), 193-205.
- Zeledon, M., Eckart, N., Taub, M., Vernon, H., Szymanski, M., Wang, R., . . . Valle, D. (2015). Identification and functional studies of regulatory variants responsible for the association of NRG3 with a delusion phenotype in schizophrenia. *Mol Neuropsychiatry*, *1*(1), 36-46. doi:10.1159/000371518
- Zhang, D., Sliwkowski, M. X., Mark, M., Frantz, G., Akita, R., Sun, Y., . . . Godowski, P. J. (1997). Neuregulin-3 (NRG3): a novel neural tissue-enriched protein that binds and activates ErbB4. *Proc Natl Acad Sci U S A*, *94*(18), 9562-9567.
- Zhou, L., Fisher, M. L., Cole, R. D., Gould, T. J., Parikh, V., Ortinski, P. I., & Turner, J. R. (2018). Neuregulin 3 Signaling Mediates Nicotine-Dependent Synaptic Plasticity in the Orbitofrontal Cortex and Cognition. *Neuropsychopharmacology*, *43*(6), 1343-1354. doi:10.1038/npp.2017.278

FIGURE LEGENDS

Figure 1. Characterization of specific Nrg3 antibodies. Antibodies were tested for their ability to recognize Nrg3 by Western blot analysis. **Panel a.** For Western blotting, detergent extracts corresponding to 50 µg of protein per lane of Neuro2a (N2a) control (**lane U**), N2a/Nrg3

(lane N3), and adult rat brain extracts (lane Br) were analyzed by SDS-PAGE using 8% Tris-glycine gels followed by Western blotting. The blots were probed with: **panel 1**, serum #6144 (1:2,000); **panel 2**, serum #6144 (1:2,000) preabsorbed with GST-Nrg3 (1.46 µg); **panel 3**, affinity-purified anti-Nrg3 (0.27 µg/ml); **panel 4**, affinity-purified anti-Nrg3 (0.27 µg/ml) preabsorbed with GST-Nrg3 (1.46 µg). **Panel b.** Anti-Nrg3 antibodies were tested for cross-reactivity against Nrg1 and Nrg2. Detergent extracts corresponding to 50 µg of protein per lane of N2a control (lane U), N2a/Nrg1 (lane N1), N2a/Nrg2 (lane N2), and N2a/Nrg3 (lane N3) were analyzed by SDS-PAGE using 4-20% Tris-glycine gels followed by Western blotting. The blots were probed with: **panel 1**, affinity-purified anti-Nrg1 (0.27 µg/ml); **panel 2**, affinity-purified anti-Nrg2 (0.28 µg/ml); and **panel 3**, affinity-purified anti-Nrg3 (0.27 µg/ml). **Panel c.** Whole brain detergent extracts corresponding to 50 µg of protein per lane of embryonic (E)18, postnatal (P) day 0, P3, P5, P7, P11, P14, P20, P28 and P50 (A), were analyzed by SDS-PAGE using 8% Tris-glycine gels followed by Western blotting. The blots were probed with affinity-purified anti-Nrg3 (0.27 µg/ml, top panel) and β-actin (1:5,000, bottom panel). **Panel d.** Detergent extracts (15 µg/lane) from E18 (**panel 1**) and P25 (**panel 2**) rat cortices were incubated overnight with or without PNGase F, EndoH, O-glycosidase (O-gly), neuraminidase (NA), or an O-gly/NA mixture (O-gly/NA). SDS-PAGE was performed using 8% Tris-glycine gels followed by Western blot analysis using affinity-purified anti-Nrg3 antibodies (0.27 µg/ml).

Figure 2. Compartmentalization of Nrg3 by immunocytochemistry. Anti-Nrg3 antibodies were used to detect the localization of Nrg3 by immunocytochemistry in the absence of (**panels a-q**) and in the presence of 0.01 % Triton X-100 (**panels a"-q"**). Immunofluorescence staining of untransfected (UNT) N2a cells (**panels a and a"**) and N2a/Nrg3 cells (**panels b-h, b"-h"**, **o-q and o"-q"**) was performed using: #6144 antisera (1:250, **panels a-c, a"-c"**, **o-q and o"-q"**); #6144 antisera (1:250) pre-absorbed with GST-Nrg3 (0.75 µg, **panels d and d"**); affinity-purified anti-Nrg3 antibodies (2.16 µg/ml, **panels f and g and f" and g"**); affinity-purified anti-

Nrg3 antibodies (2.16 µg/ml) pre-absorbed with GST-Nrg3 (0.75 µg, **panels h and h''**) and secondary antibodies only (1:300, **panels e and e''**). N2a cells shown in **panels i-q and i''-q''** were transfected with either NRG1, 2 or 3 and co-transfected with an mCherry encoding plasmid. N2a/Nrg1/mCherry (**panels i-k and i''-k''**) and N2a/Nrg2/mCherry cells (**panels l-n, and l''-n''**) was performed using: #6144 antisera (1:250). The mCherry expressing cells appear in magenta. Anti-Nrg3 antibodies were detected using secondary antibodies coupled to Alexa Fluor 488 (in green). The nuclei were visualized using either DAPI, (**panels a-h and a''-h''**) or Hoechst 33342 (**panels i-q and i''-q''**) (both in blue). Scale bar = 15 µm for all panels.

Figure 3. Nrg3 is enriched in the Golgi apparatus. Double immunofluorescent staining using serum #6144 antiserum (1:250, **panels a, d, and h**) and anti-GM-130 (1:500, **panels b, e, and i**) was performed on N2a/Nrg3 transfected cells (**panels a-c**), cortical neurons expressing endogenous Nrg3 (**panels d-g**), and cerebral cortex coronal sections (15 µm) of P7 rats expressing endogenous Nrg3 (**panels h-k**). Merged images are shown in **panels c, f, j and k**. Cortical neurons (**panel g**) and cerebral cortex coronal sections (15 µm) of P7 rats (**panel k**) were stained with secondary antibodies only (1:300). Arrows in **panels a-c** point to N2a untransfected cells that were negative for Nrg3 but stained with anti-GM-130. For all panels the staining was performed in the presence of 0.01% Triton X-100 detergent. Anti-GM-130 antibodies were detected with anti-mouse secondary antibodies coupled with AlexaFluor 594 (in magenta) and anti-Nrg3 antibodies were detected using anti-rabbit secondary antibodies coupled to Alexa Fluor 488 (in green) both at 1:300 dilution. The nuclei were visualized using DAPI (in blue). Scale bar = 15 µm for all panels.

Figure 4. Expression of Nrg3 in neurons. Dissociated cortical cell cultures (8 days *in vitro*) (**panels a-c and g-i**) and 15 µm coronal sections of P4 (**panels d-f and j-l**) and P7 rat brain (**panels m-o**) were double stained with Nrg3 #6144 antiserum (1:250, **panels a, d, g, j and m**),

and with anti-MAP2 antibodies (1:1,000, **panels b and e**), anti-GAD-6 antibodies (1:25,000, **panels h and k**) or anti-parvalbumin (1:1,000, **panel n**) in the presence of 0.01% Triton-X 100 (all panels). The anti-Nrg3 antibodies were visualized with AlexaFluor 488 goat anti-rabbit antibodies (in green) and the anti-MAP2, anti-GAD-6, and anti-parvalbumin antibodies with AlexaFluor 594 goat anti-mouse antibodies (in magenta) both at 1:300 dilution. The nuclei were visualized using DAPI (in blue). Scale bar = 15 μ m for all panels

Figure 5. Expression of Nrg3 in glia. Dissociated cortical cell cultures (8 days *in vitro*) (**panels a-c and g-i**), 15 μ m coronal sections of P3 rat brain (**panels d-f**), and 15 μ m coronal sections of P7 rat brain (**panels j-l**), were double stained with Nrg3 #6144 antiserum (1:250, **panels a, d, g, and j**), with anti-GFAP (1:500, **panels b and e**), anti-O4 antibodies (1:1,000, **panel h**), and anti-CNPase (1:500, **panel k**) in the presence of 0.01% Triton X-100 for all panels. The anti-Nrg3 antibodies were visualized with AlexaFluor 488 goat anti-rabbit antibodies (in green) and anti-GFAP, anti-O4, and anti-CNPase antibodies were visualized with AlexaFluor 594 goat anti-mouse antibodies (in magenta) both at 1:300 dilution. The nuclei were visualized using DAPI (in blue). Scale bar = 15 μ m for all panels.

Figure 6. Overall distribution of Nrg3 mRNA by *in situ* hybridization. *In situ* hybridization was performed using antisense probes for Nrg3 mRNA in 30 μ m sagittal sections of E19 (**panel j**) and P20 rat brain (**panel k**) and in coronal sections of P7 rat brain (**panels a-i**). Abbreviations in alphabetical order: 7, facial nucleus; AA, anterior amygdaloid area; AON, anterior olfactory nucleus; Aq, aqueduct; BLA, basolateral amygdaloid nucleus; BMA, basomedial amygdaloid nucleus; CA1, CA1 field of the hippocampus; CA3, CA3 field of the hippocampus; CPu, caudate-putamen; Cb, cerebellum; ChP, choroid plexus; Cg, cingulate cortex; cc, corpus callosum; Cx, cortex; CxP, cortical plate; DG, dentate gyrus; DEn, dorsal endopiriform nucleus; Fr, frontal cortex; Gl, glomerular layer of the olfactory bulb; GL, granule cell layer; Hi,

hippocampus; IC, inferior colliculus; ic, internal capsule; IZ, intermediate zone; IGr internal granule layer of the olfactory bulb; CerN, cerebellar nucleus; LH, lateral hypothalamic area; LP, lateral posterior nucleus of the thalamus; LSN, lateral septal nucleus; LV, lateral ventricle; Mhb, medial habenula; MD, mediodorsal thalamic nucleus; mcp, middle cerebellar peduncle; Mi, mitral cell layer of the olfactory bulb; Orb, orbital cortex; Pir, piriform cortex; Pn, pontine nuclei; PLCo, posteromedial amygdaloid nucleus; PCL, Purkinje cell layer; SN, substantia nigra; SVZ, subventricular zone; SC, superior colliculus; TT, tenia tecta; Th, thalamus; VCA, ventral cochlear nucleus; VPM, ventral posteromedial nucleus of the thalamus; VL, ventrolateral nucleus of the thalamus; VMH, ventromedial hypothalamic nucleus; VP, ventroposterior nucleus of the thalamus; wm, cerebellar white matter. Scale bar = 125 μm for a and j; 160 μm for b-i and k.

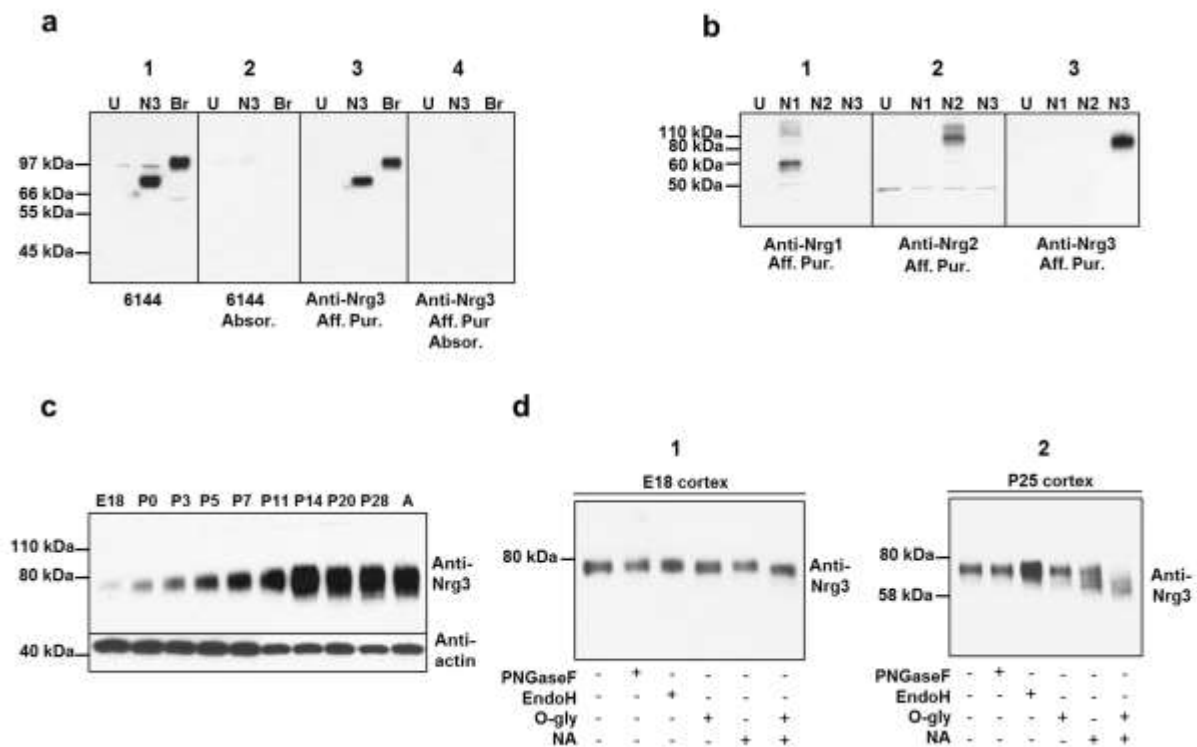
Figure 7. Nrg3 expression in the cerebral cortex. *In situ* hybridization was performed using antisense probes for Nrg3 mRNA on 30 μm parasagittal sections of E17 (**panel a**), coronal sections of P3 (**panel h**) and P7 (**panel j**). Immunofluorescent staining was performed on 15 μm parasagittal sections of E17 (**panel b-g**) rat brain, and coronal sections of P3 (**panel i**) and P7 (**panel k**) cerebral cortices. The immunofluorescence staining was performed with Nrg3 #6144 antiserum (1:250, **panels b-e, g, i and k**) and anti-MAP2 (1:1,000, **panel f**) in the presence of 0.01% Triton X-100. The anti-Nrg3 antibodies were visualized with AlexaFluor 488 goat anti-rabbit antibodies (in green) and MAP2 antibodies were visualized with AlexaFluor 594 goat anti-mouse antibodies (in magenta) both at 1:300 dilution. Abbreviations in alphabetical order: CPu, caudate-putamen; Cx, cortex; CxP, cortical plate; Gl, glomerular layer of the olfactory bulb; IZ, intermediate zone; LV, lateral ventricle; MZ, marginal zone; SP, subplate; SVZ, subventricular zone; V, ventricle; VZ, ventricular zone. Scale bar= 100 μm for a; 50 μm for b-f, h and j; 220 μm for g; and 175 μm for i.

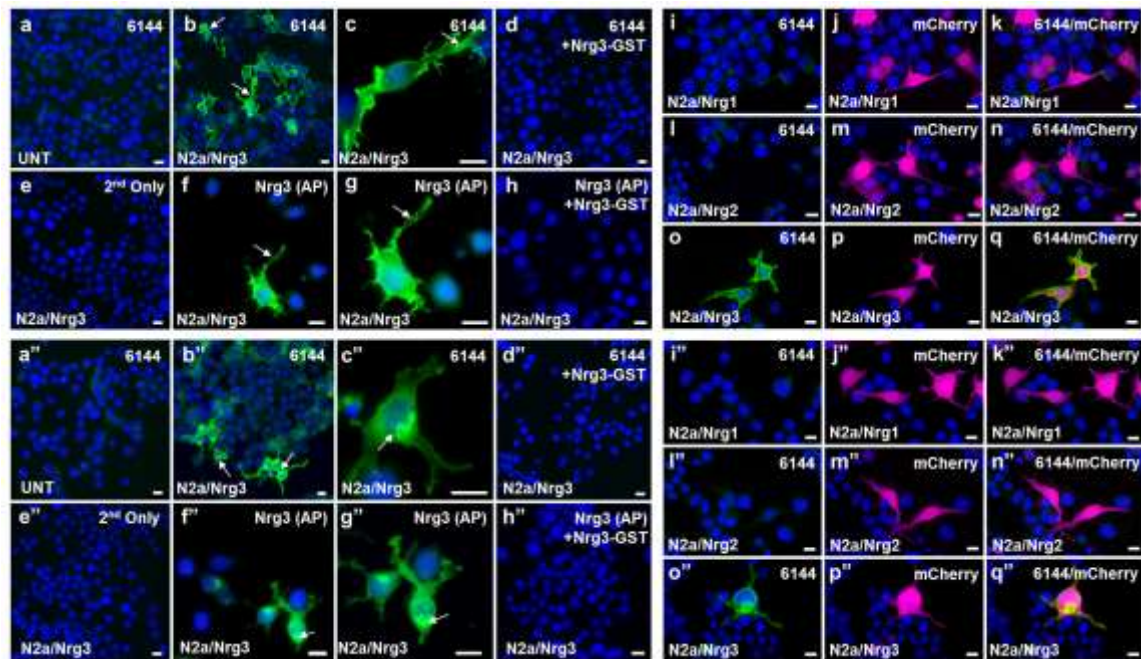
Figure 8. Developmental expression of Nrg3 in the cerebellum. *In situ* hybridization was performed using antisense probes for Nrg3 (**panels a, b, and d**) or Nrg1 type III mRNA (**panel c**) in 30 μm coronal sections of P3 (**panel a**), P7 (**panels b and c**), or parasagittal P20 sections (**panel d**). Immunofluorescent staining was performed on 15 μm coronal sections of P7 (**panels e-g**) or sagittal sections of P20 (**panel h**) rat brains using Nrg3 #6144 antiserum (1:250, **panels e and h**), anti-calbindin (calb) antibodies (1:1,000, **panels f and g**) or anti-GFAP antibodies (1:500, **panel h**) in the presence of 0.01% Triton X-100 for all panels. The anti-Nrg3 antibodies were visualized with AlexaFluor 488 goat anti-rabbit antibodies (in green) and anti-calbindin and anti-GFAP antibodies were visualized with AlexaFluor 594 goat anti-mouse antibodies (in magenta) both at 1:300 dilution. Abbreviations: BG, Bergman glia; EGL, external granule cell layer; IGL, internal granule cell layer; ML, molecular layer; PC, Purkinje cell. Scale bar = 160 μm for a and b; 200 μm for c and d; and 15 μm for e-h.

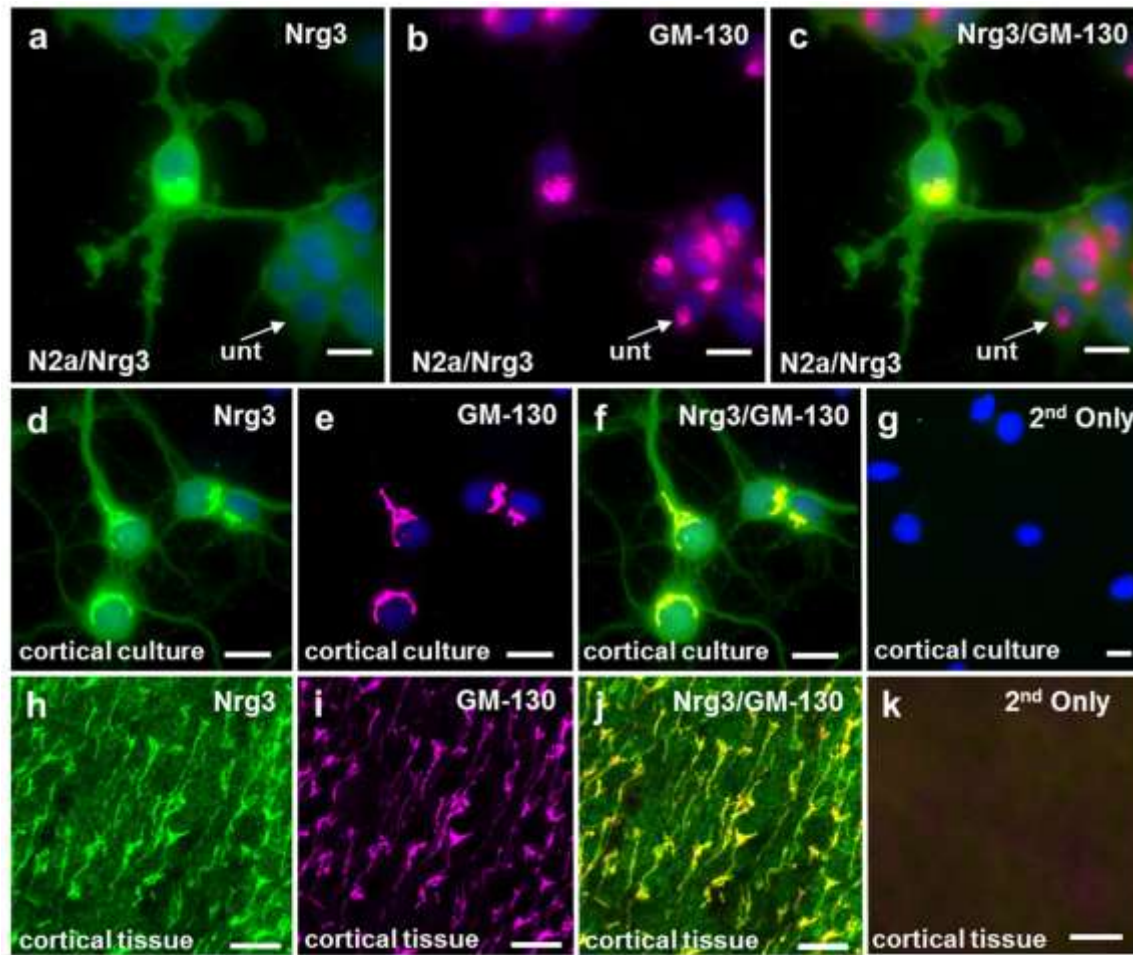
Figure 9. Nrg3 expression in the hippocampal formation. *In situ* hybridization was performed using antisense probes for Nrg3 mRNA in 30 μm coronal sections of P3, P7, and P25 rat brains (**panels a--c respectively**). Immunofluorescent staining was performed on 15 μm coronal sections of P3 (**panels d and f**) and P7 (**panels e and g**) rat brains with Nrg3 #6144 antiserum (1:250) in the presence of 0.01% Triton X-100 for all immunofluorescent staining. The anti-Nrg3 antibodies were visualized with AlexaFluor 488 goat anti-rabbit antibodies (in green) both at 1:300 dilution. Abbreviations: CA1, CA1 field of the hippocampus; CA3, CA3 field of the hippocampus; DG, dentate gyrus. Scale bar = 80 μm for a and b; 100 μm for c; and 15 μm for d-g.

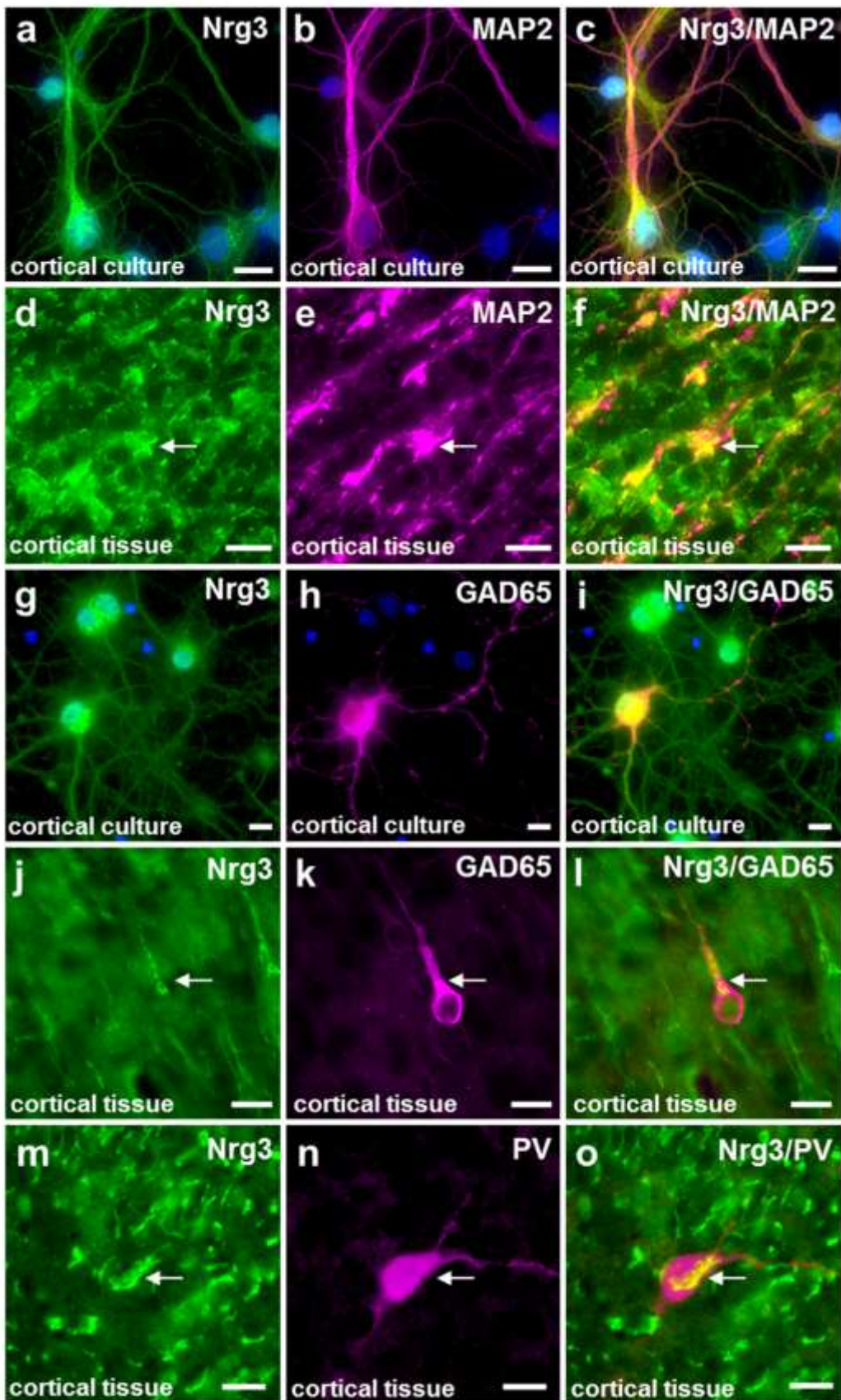
Figure 10. Overall distribution of Nrg3 mRNA. *In situ* hybridization was performed using antisense probes against Nrg1 type III (**panels a-c**), Nrg2 (**panels d-f**), and Nrg3 mRNAs (**panels g-i**) in 30 μm coronal sections of P7 rat brain. Abbreviations in alphabetical order: 7,

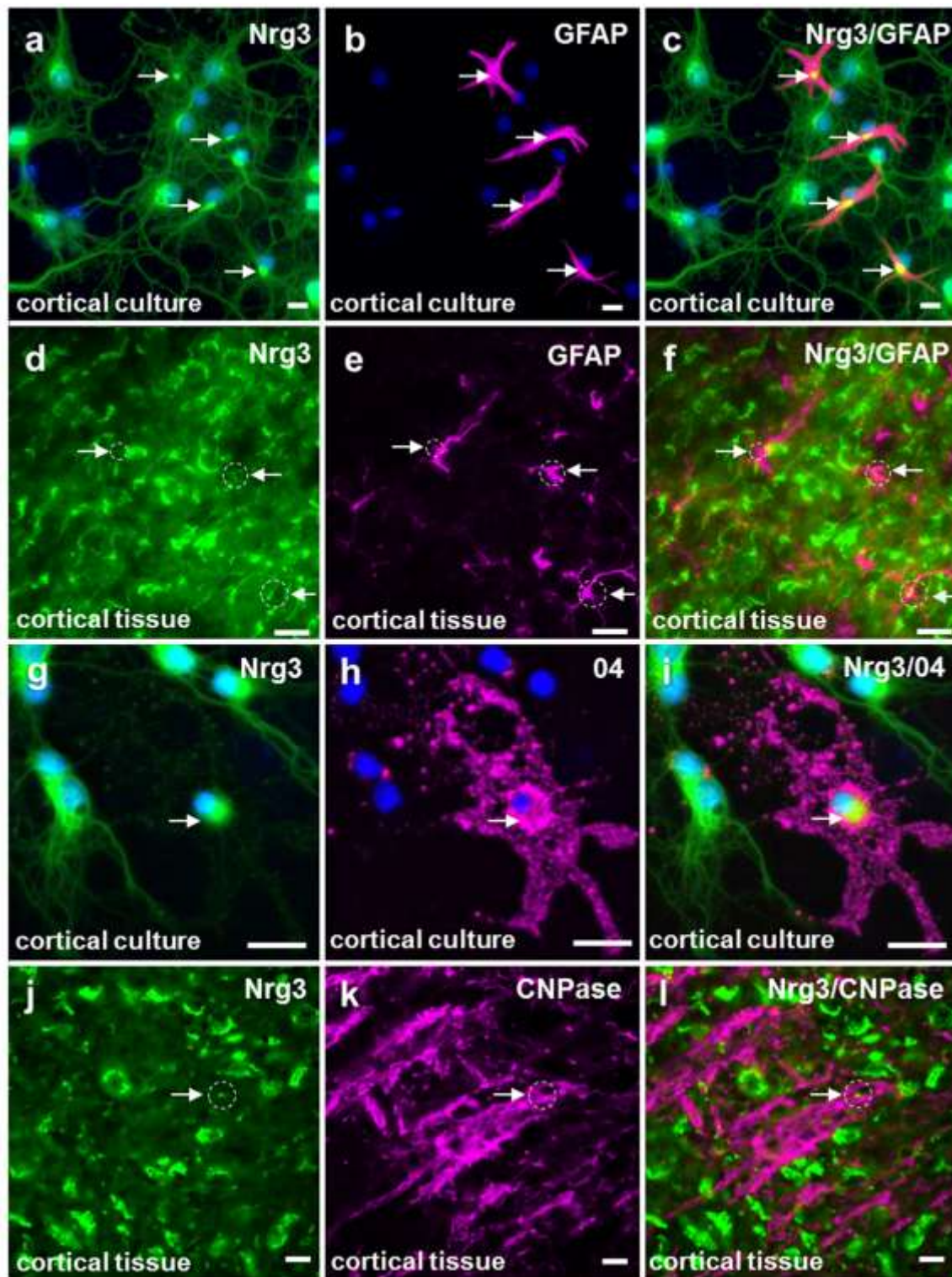
facial nucleus; Arc, arcuate hypothalamic nucleus; BLA, basolateral amygdaloid nucleus; CA1, CA1 field of the hippocampus; CA3, field of the hippocampus; CPu, caudate-putamen; cc, corpus callosum; Cx, cortex; lv, cortical layer V; DG, dentate gyrus; IC, inferior colliculus; IGL, internal granule cell layer; Mhb, medial habenula; MS, medial septal nucleus; Pa, paraventricular hypothalamic nucleus; pir, piriform cortex; PLCo, posteromedial amygdaloid nucleus; PCL, Purkinje cell layer; Rt, reticular nucleus of the thalamus; SN, substantia nigra; TT, tenia tecta; VCA, ventral cochlear nucleus; VPL, ventral posterolateral nucleus of the thalamus; VPM, ventral posteromedial nucleus of the thalamus. Scale bar = 160 μ m for a and i; and 200 μ m for b-h.

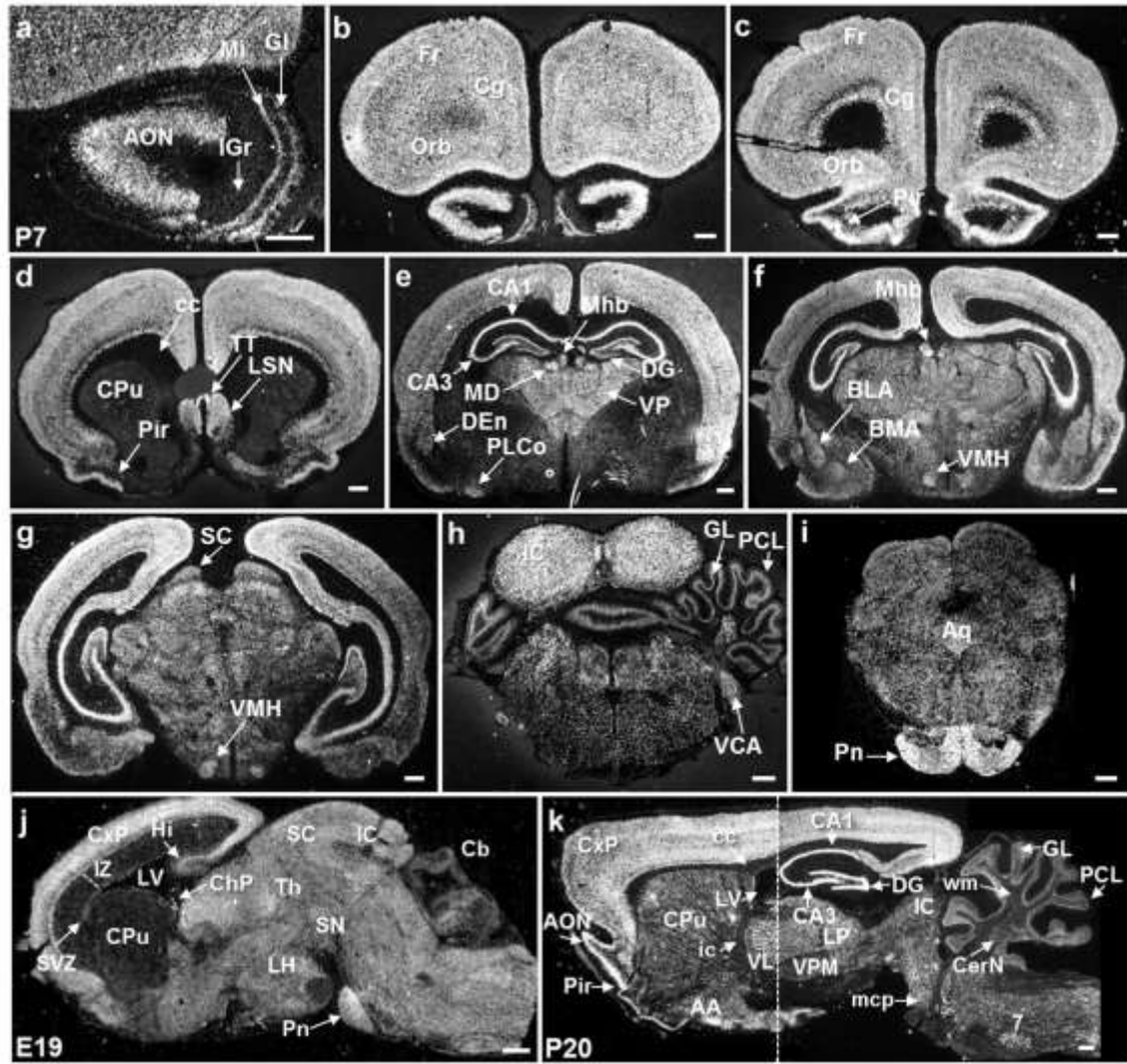


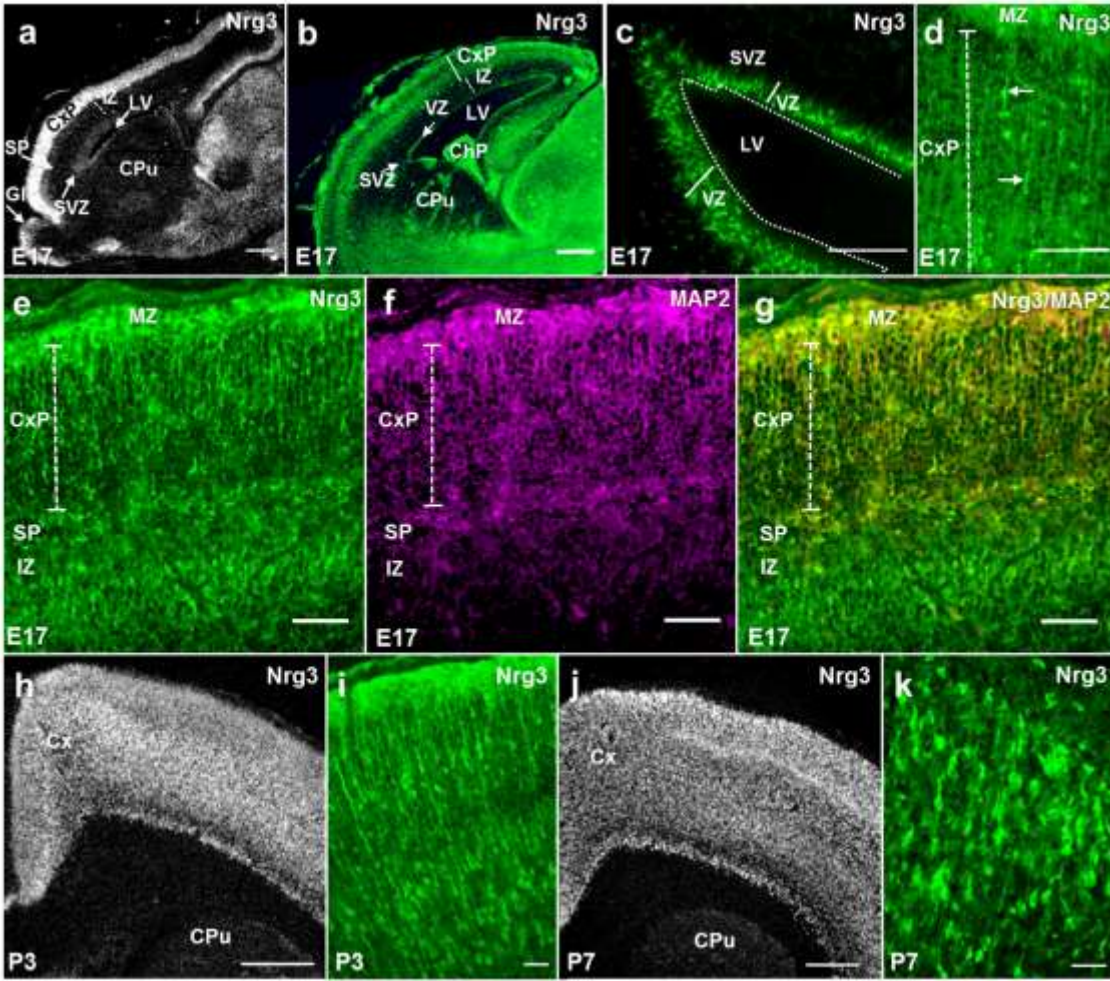


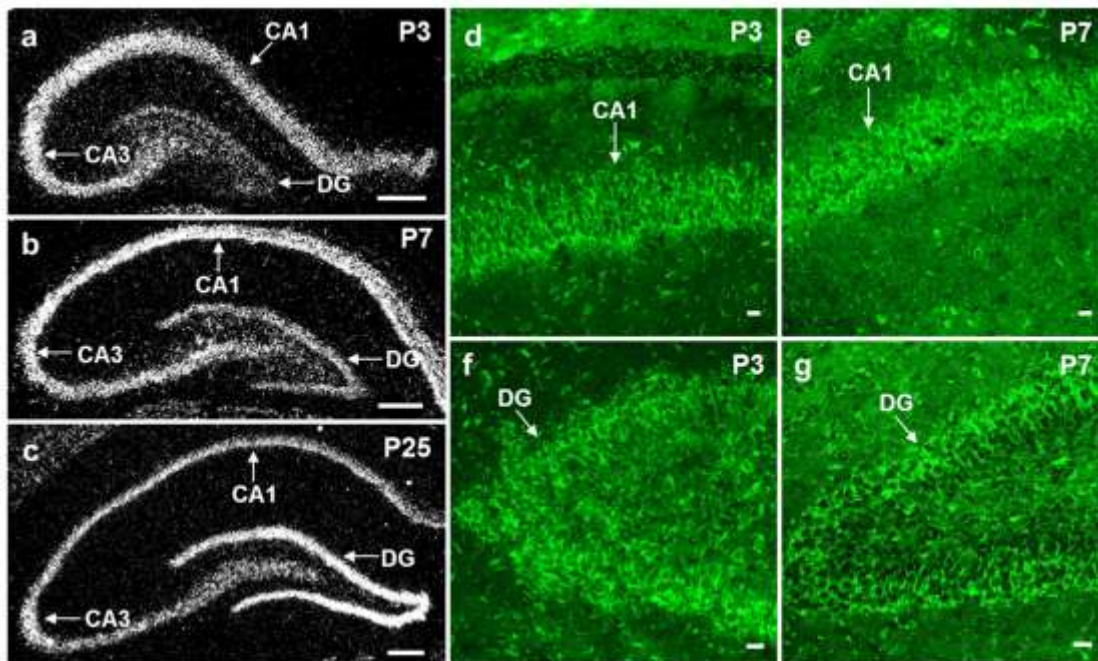
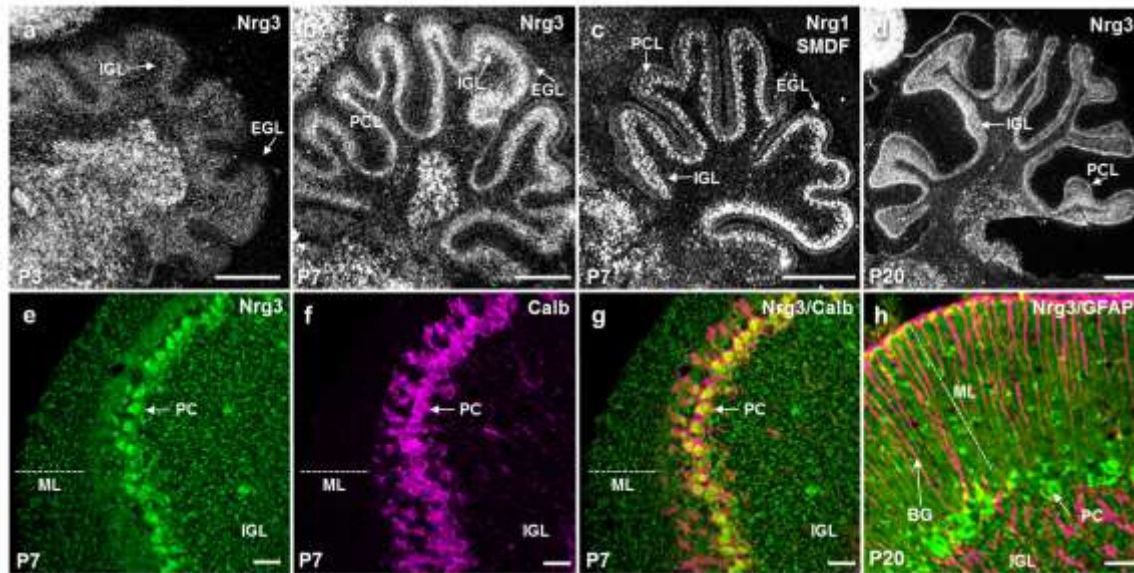


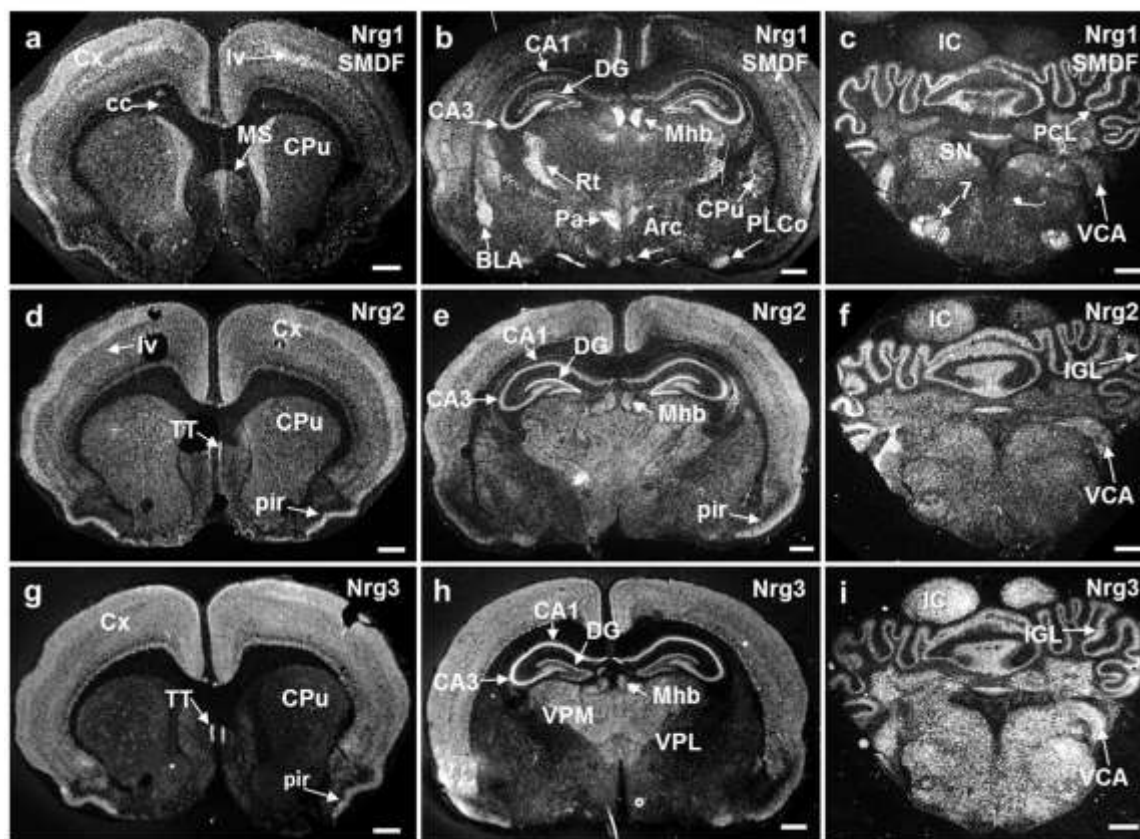












The schizophrenia risk factor, Neuregulin-3 is O-linked glycosylated and enriched in the plasma membrane and Golgi apparatus in neurons, including GABAergic interneurons. It is more widely distributed than other NRGs in the rat brain and highly expressed in the cerebral cortex, olfactory bulb, the thalamus, hippocampus cerebellum and brain stem.

